

RSC Advances



This is an *Accepted Manuscript*, which has been through the Royal Society of Chemistry peer review process and has been accepted for publication.

Accepted Manuscripts are published online shortly after acceptance, before technical editing, formatting and proof reading. Using this free service, authors can make their results available to the community, in citable form, before we publish the edited article. This *Accepted Manuscript* will be replaced by the edited, formatted and paginated article as soon as this is available.

You can find more information about *Accepted Manuscripts* in the [Information for Authors](#).

Please note that technical editing may introduce minor changes to the text and/or graphics, which may alter content. The journal's standard [Terms & Conditions](#) and the [Ethical guidelines](#) still apply. In no event shall the Royal Society of Chemistry be held responsible for any errors or omissions in this *Accepted Manuscript* or any consequences arising from the use of any information it contains.

Does surface coating of metallic nanoparticles modulate their interferences with *in vitro* assays?

Ivana Vinković Vrček^{a,*}, Ivan Pavičić^a, Tea Crnković^b, Darija Jurašin^c, Michal Babič^d, Daniel Horák^d, Marija Lovrić^e, Lejla Ferhatović^e, Marija Ćurlin^e, Srećko Gajović^e

^a Institute for Medical Research and Occupational Health, Ksaverska cesta 2, 10 000 Zagreb, Croatia

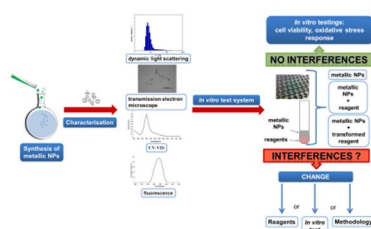
^b Faculty for Pharmacy and Biochemistry, University of Zagreb, Ante Kovačića 1, 10 000 Zagreb, Croatia

^c Division of Physical Chemistry, Ruđer Bošković Institute, Bijenička cesta 54, 10 000 Zagreb, Croatia

^d Institute of Macromolecular Chemistry, Academy of Sciences of the Czech Republic, Heyrovský Sq. 2, 162 06 Prague 6, Czech Republic

^e School of Medicine, Croatian Institute for Brain Research, University of Zagreb, Šalata, 10 000 Zagreb, Croatia

* Corresponding author. E-mail address: ivinkovic@imi.hr. Tel.: +385 1 4682540; fax: +385 1 4673303



Experimental setup for *in vitro* evaluation of metallic nanoparticles where interferences depend on metal core, surface coating, and the test system.

ABSTRACT

Screening programs for the evaluation of nanomaterial value and safety rely on *in vitro* tests. The exceptional physicochemical properties of metallic nanoparticles (NPs), such as large surface area and chemically active surface, may provoke their interferences with *in vitro* methods and analytical techniques used for evaluation of biocompatibility or toxicity of NPs. This study aimed to determine if such interferences could be predicted on the basis of the surface characteristics of metallic NPs by investigating the effect of different surface coatings of silver (AgNPs) and maghemite NPs (γ -Fe₂O₃NPs) on common *in vitro* assays scoring two of the main cytotoxic endpoints: cell viability and oxidative stress response. We examined optical, adsorptive and chemically reactive types of NPs interferences with cell viability assays (MTT, MTS, and WST-8) and assays employing fluorescent dyes as markers for production of reactive oxygen species (DCFH-DA and DHE) or glutathione level (MBCl). Each type of tested NPs affected all of the six investigated assays leading to false interpretation of obtained results. The extent and type of interference were dependent on the type and surface coating of NPs as well as on their stability in biological media. The results have shown that interferences were concentration-, particle type- and assay type-dependent. This study demonstrated that common *in vitro* assays, without appropriate cause-and-effect analysis and adaptation or modification, are ineffective in the evaluation of biological effects of metallic NPs due to their interaction with optical readouts and assay components. A comprehensive and feasible experimental setup has been proposed to gain a reproducible and reliable *in vitro* evaluation as the first step in the health assessment of metallic NPs.

Keywords: nanoparticles, silver, maghemite, *in vitro* assay, interferences, cell viability, oxidative stress

Introduction

Recent medical and commercial uses of metals employ them in the form of nanoparticles (NPs). The unique physicochemical properties and increased reactivity of NPs lead to rapid commercialization and use of NP-based consumer products. For biomedical uses, there is well-known application of metallic NPs like maghemite nanoparticles ($\gamma\text{-Fe}_2\text{O}_3\text{NPs}$) and silver nanoparticles (AgNPs). $\gamma\text{-Fe}_2\text{O}_3\text{NPs}$ are the commonly investigated for current applications in magnetic resonance imaging, multimodal imaging, thermo-therapy, drug delivery, gene therapy, biomolecular separation.¹ Silver NPs have found their use in biomedicine, water and air purification, food contact materials, clothing, and numerous household products due to their excellent antimicrobial properties.² The worldwide production of AgNPs is estimated to be more than 300 tons per year.³ AgNPs have also received considerable attention in biomedical imaging as promising candidates for molecular labelling in surface enhanced Raman scattering, due to their surface plasmon resonance and large effective scattering cross-section of individual AgNPs.⁴ Given the potential clinical uses of these NPs, the evaluation of their biocompatibility and safety is highly important.

The current biomedical verification of metallic NPs is based on *in vitro* screening to help elucidate the mechanism of their interactions with cellular systems and consequences of their action *in vivo*. There are a number of advantages of *in vitro* toxicity assays, although there are not able to fully encounter all complex interactions that occur between multiple cell types *in vivo*. Most *in vitro* assays are plate-reader based with optical readouts of luminescence, absorbance, fluorescence, time-resolved fluorescence or fluorescence polarization.⁵ They are easy to perform, control and interpret, reduce animal testing, and the results are available within a short time. Therefore, *in vitro* assessment is expected to be a core component of any screening program to understand the biological effects of different NPs.⁶⁻⁷ However, such

studies should ideally be designed to avoid any undesirable interactions and side effects influenced by nanospecific properties.^{8,9}

Unique physicochemical properties of NPs such as high adsorption capacity, hydrophobicity, surface charge, optical and magnetic properties, or catalytic activity may interfere with assay components and/or detection systems used by *in vitro* methods.^{2,5-10} In last decade, an increasing number of studies have evidenced data artefacts resulting from NPs interferences with light absorption or fluorescence used for detection in assays, uncontrolled chemical reactions, or adsorption of assay compounds to the NP surfaces.¹¹⁻³⁰ Simply performing *in vitro* toxicity assays for NPs according to the manufacturers' recommendations can lead to underestimations or overestimations of toxicity.¹³⁻¹⁸ It has been reviewed that engineered NPs interfere with classic cytotoxicity assays in a concentration-, particle- and assay-specific manner.⁷⁻¹⁰ Consequently, testing NPs with established and commercial assays represents a challenge requiring careful analysis and evaluation of the assay system and data obtained. Recent investigations have identified key issues that need to be addressed for improving the accuracy of nanotoxicity assessments.⁵⁻³⁰ There are a number of criteria that have been proposed how to integrate and avoid interferences with testing systems;^{8-10,13-18,21-23} i.e. a careful selection of the test systems and suitable methods that have to be established and validated, well-characterized NPs, the use of available reference materials, behavioural information of each NP type and its dispersions, inclusion of a range of relevant controls, use of systematic approaches to prevent misinterpretation of data. All these studies⁷⁻³⁰ strongly suggest that each *in vitro* test system has to be evaluated for each single NP type to accurately assess the nanoparticle toxicity.

Therefore, NPs compatibility with *in vitro* assay is a very important requirement with a dramatic impact on the validity of the results and consequently outcome of safety assessment of nanomaterials.⁹ However, possible interferences between NPs and the assay system are

difficult to predict in advance, as they can be dependent on the chemical composition, particle size, shape, surface structure, surface charge, and stability parameters in dispersion media.⁷⁻¹⁰

Although metal-based NPs were already described to interfere with *in vitro* assays,¹⁴⁻²¹ this study is the first comprehensive evaluation of different AgNPs and γ -Fe₂O₃NPs. The most recently published paper reported NP-assay interferences varying by multiple physicochemical properties and chemical composition, and only rarely by the effect of a single property (mainly size) of the same NPs type.

Therefore, this study aimed: 1) to predict the role of surface coating of metallic NPs on their interferences with conventional *in vitro* assays, and 2) to assess the reliability and limits of *in vitro* assays in the biocompatibility evaluation of metallic NPs. We chose two types of metallic NPs, AgNPs and γ -Fe₂O₃-NPs. Each type was of similar size and obtained by the same production process, and stabilized with different surface coating. We selected the most common *in vitro* assays that determine 2 different cytotoxic endpoints: metabolic activity and oxidative stress (Table 1). A systematic investigation of assay interferences imparted by well-characterized NPs was performed in the cell-free culture medium using a set of 7 silver NPs, coated with trisodium citrate (CITAgNP), sodium bis(2-ethylhexyl)-sulfosuccinate (AOTAgNP), cetyl trimethylammonium bromide (CTAAgNP), poly(vinylpyrrolidone) (PVPAgNP), poly-L-lysine (PLLAgNP), Brij 35 (BrijAgNP) and Tween 20 (TweenAgNP), and 3 maghemite NPs, uncoated γ -Fe₂O₃-NPs (UN γ -Fe₂O₃NPs), and coated with *D*-mannose (MAN γ -Fe₂O₃NPs) and poly-L-lysine (PLL γ -Fe₂O₃NPs). For each of the six different *in vitro* assays, we tested possible NPs interferences with optical readouts used for detection as well as interactions between NPs and components used for each assay. Then, representative assays (WST-8 and DCFH-DA) were evaluated for measuring NPs effects on human hepatoma (HepG2) cells by implementing experimental setup developed within this project. This setup,

schematically presented in Figure 1, is based on a well-known cause-and-effect analysis,³¹ proposed already as a core element of nanotoxicological assessments.¹³

Materials and methods

Chemicals and materials

If not otherwise stated, all of the chemicals were obtained from Sigma-Aldrich Chemie GmbH (Munich, Germany). Phenol red-free Dulbecco's modified Eagle's medium (DMEM) was obtained from Lonza (Verviers, Belgium). MTT Cell Proliferation Assay was purchased from American Type Culture Collection (Manassas, USA). CellTiter 96[®] AQueous One Solution Cell Proliferation Assay was obtained from Promega (Madison, USA). Cell Counting Kit - 8 was purchased from Sigma-Aldrich. The plastic and glassware used for chemical analysis and cell culturing were from Sarstedt (Belgium). Osmium tetroxide was purchased from Agar Scientific (Stansted, UK) and TAAB epoxy resin (medium hard) from Aldermaston (Berkshire, UK). All dilutions were made with ultrapure water (18.2 MΩcm), obtained from a GenPure UltraPure water system (TKA Wasseraufbereitungssysteme GmbH, Niederelbert, Germany).

Synthesis and characterization of metallic nanoparticles

Seven different AgNPs were synthesized by the chemical reduction of silver nitrate (briefly described in Supporting Information (SI)) and stabilized with structurally diverse surface coatings – trisodium citrate (CITAgNP), sodium bis(2-ethylhexyl)-sulfosuccinate (AOTAgNP), cetyl trimethylammonium bromide (CTAAgNP), poly(vinylpyrrolidone) (PVPAgNP), poly-*L*-lysine (PLLAgNP), Brij 35 (BrijAgNP), and Tween 20 (TweenAgNP). Immediately after synthesis, freshly prepared NP suspensions were washed twice with

ultrapure water (UPW) using centrifugation at $15790 \times g$ for 20 min. The washed AgNPs were resuspended in UPW using ultrasound, and stored in the dark at 4 °C until use. Total silver concentrations in AgNPs colloidal suspensions were determined in acidified solutions (10% HNO₃) using an Agilent Technologies 7500cx inductively coupled plasma mass spectrometer (ICPMS) (Waldbronn, Germany). A silver standard solution (1000 mg/L in 5% HNO₃) from Merck (Darmstadt, Germany) was used for calibration.

Three different maghemite nanoparticles (γ -Fe₂O₃NPs) - uncoated, coated with poly-*L*-lysine and *D*-mannose - were prepared according to methods described previously.³² Shortly, coprecipitation of FeCl₂ and FeCl₃ was achieved by increasing the pH with ammonium hydroxide, followed by the oxidation of the resulting magnetite with sodium hypochlorite.³³ Obtained maghemite (γ -Fe₂O₃) was referred as uncoated γ -Fe₂O₃NPs (UN γ -Fe₂O₃NPs). The post-synthesis coating of maghemite with *D*-mannose (MAN γ -Fe₂O₃NPs) or poly-*L*-lysine (PLL γ -Fe₂O₃NPs) was achieved³³ by addition of *D*-mannose or poly-*L*-lysine to the primary uncoated maghemite cores.³⁴

The formation of nanosized metallic particles was verified by the presence of a Surface Plasmon Resonance (SPR) peak measured using an UV-Vis spectrophotometer (CARY 300, Varian Inc., Australia). Careful characterization of each NP type (concentration 10 mg/L) was conducted in both UPW and phenol-red free DMEM as cell-free culture medium (CCM). The aim was to ascertain whether there is a time-dependent agglomeration of NPs at various incubation times in two different media, since the properties of agglomerated and individual NPs may significantly differ. The size and charge of NPs were measured at 25 °C by dynamic (DLS) and electrophoretic light scattering (ELS) at 173° using Zetasizer Nano ZS (Malvern, UK) equipped with a green laser (532 nm). To avoid overestimations arising from the scattering of larger particles, the hydrodynamic diameter (d_H) was obtained as a value at peak

maximum of size volume distribution function. Size values are reported as an average of 10 measurements. The charge of the NPs was characterized by zeta (ζ) potential values, which was calculated from the measured electrophoretic mobility by means of the Henry equation using the Smoluchowski approximation. Each sample was measured 5 times and the results are expressed as average value. The data were processed by the Zetasizer software 6.32 (Malvern Instruments). In addition, particles were visualized using a transmission electron microscope (TEM, Zeiss 902A) operated in bright field mode at an acceleration voltage of 80 kV. Images were recorded with Canon PowerShot S50 camera attached to the microscope. TEM samples were prepared by depositing a drop of the particle suspension on a Formvar[®] coated copper grid and air-drying at room temperature.

Cell viability assays

Three different cell viability assays were tested: MTT, MTS, and WST-8. All three assays use tetrazolium salts that can be bio-reduced by dehydrogenases in metabolically active cells to a soluble formazan product. The quantity of formazan is indicative of the number of viable cells in culture and can be determined spectrophotometrically. The MTT cell proliferation assay determines cellular metabolic activity by the reduction of the yellow tetrazolium salt MTT (3-(4,5-dimethylthiazol-2-yl)-2,5-diphenyltetrazoliumbromide) to a purple MTT-formazan crystal. To dissolve the MTT-formazan crystals, DMSO was added and the quantity of MTT-formazan was determined spectrophotometrically at 590 nm. The MTS cell viability assay (Cell Titer 96[®] Aqueous Non-Radioactive Cell Proliferation Assay Kit) uses MTS (3-(4,5-dimethylthiazol-2-yl)-5-(3-carboxymethoxyphenyl)-2-(4-sulfo-phenyl)-2H-tetrazolium) that can be bio-reduced to a soluble MTS-formazan product which can be determined by recording the absorbance at 490 nm. The WST-8 assay (Cell Counting Kit-8) utilizes the water-soluble tetrazolium salt WST-8 (2-(2-methoxy-4-nitrophenyl)-3-(4-nitrophenyl)-5-(2,4-

disulfophenyl)-2H-tetrazolium) which produces a water-soluble formazan dye. The quantity of WST-8 formazan can be determined spectrophotometrically at 450 nm.

Evaluation of NPs interferences with cell viability assays

The tendency of each NP type to interfere with particular *in vitro* assay was measured in a cell-free system. For each experiment, controls were included by measuring absorbance of NPs in the absence of any reagent. Additional controls including kit reagents in the absence of NPs were employed. The first series of experiments were performed in a cell-free culture medium (CCM) according to the manufacturer's instruction. Each NP type was loaded at different concentrations onto 96-well plates and the absorbances were measured using a Victor™ plate reader (Perkin Elmer, MA, USA). Final NP dilutions in 96-well plates were prepared immediately before measurements from the stock dispersion in UPW (1 g/L). Each measurement was performed at least in quintuplicate within the plate.

The second series of experiments was performed according to the manufacturer's instruction, but with an additional step. After incubation of NPs with kit reagents for 3 h at 37 °C in the CCM and addition of dimethyl sulfoxide (DMSO) in the case of MTT assay, the mixture was centrifuged at $1020 \times g$ for 10 min, the supernatants were transferred into new 96-well plates and the absorbances were measured on a plate reader.

In the third series of experiments, a formazan production was simulated by addition of a reducing agent. After 3 h incubation of NPs with kit reagents in the CCM, ascorbic acid (AsA, 0.05 mM) was added and incubated for another hour at 37 °C. In the MTT assay, DMSO was added at a ratio of 2:1 v/v and incubated another 10 min at 37 °C. The absorbance was measured before and after centrifugation. Additional controls were included by incubating NPs first without kit reagents, and subsequently with AsA to check possible interactions between the different NPs and AsA.

Oxidative stress assays

All three assays for the oxidative stress detection evaluated in this study (Table 1) utilize fluorescent molecular probes: 2',7'-dichlorofluorescein-diacetate (DCFH-DA), dihydroethidium (DHE) and monochlorobimane (MBCl).

The DCFH-DA assay is based on the oxidation of 2',7'-dichlorofluorescein (DCFH) dye by different types of reactive oxygen species (ROS). DCFH is applied as diacetate (DCFH-DA) which is easily taken up by the cells. The cleavage of lipophilic group occurs intracellularly by unspecific esterases.¹⁸ The resulting DCFH is nonfluorescent until oxidized by ROS to highly fluorescent 2',7'-dichlorofluorescein (DCF). In acellular systems, DA cleavage can be achieved chemically using sodium hydroxide (as in the present study) or media. The excitation of the DCF at 485 nm emits green fluorescence at 520 nm with intensity proportional to the amount of ROS.

DHE is another widely used probe for detection of intracellular ROS production. In the presence of a superoxide radical, DHE is oxidized to 2-hydroethidium (EOH) and intermediate products. These intermediate products can react with hydroxyl radical or hydrogen peroxide to form ethidium (E) to a much lesser extent.³⁵ Whereas E fluorescence is measured at excitation of 500–530 nm and emission of 590–620 nm, the EOH fluorescence is measured at an excitation and emission wavelength of 480 and 567 nm, respectively (Chen et al., 2013). EOH is stable within the cell, allowing for precise measurement of DHE fluorescence without risk of intraconversion variability.

MBCl is a cell-permeable dye which reacts exclusively with glutathione (GSH) to generate a highly fluorescent adduct that can be measured using excitation and emission wavelengths of 380 and 460 nm, respectively.³⁶ GSH is an important marker of oxidative stress, active in non-enzymatic oxidant defence mechanisms.

Evaluation of NPs interferences with oxidative stress assays

All experiments utilizing fluorescent molecular probes were carried out in 96-well black Costar plates with a clear bottom (Corning Inc., Corning, NY) to minimize fluorescence interference between wells. The fluorescence readings were taken from the top of the wells (top read). Both fluorescent probes and NPs dispersed in UPW or CCM (100 μ l per well) at defined concentrations were used as controls for each assay. Final NP dilutions in 96-well plates were prepared immediately before measurements from the stock dispersion in UPW (1 g/L).

To test the interferences of NP dispersions with the DHE assay, different concentrations of NPs dispersed in UPW or CCM were mixed with 10 μ M DHE in 96-well plates. Fluorescence was recorded five times, immediately after mixing and after 15, 30, 45 and 60 min of incubation at 37 °C with fluorescence excitation and emission at 485 and 520 nm, respectively. Each experiment was repeated at least three times with five replications. The effect of NPs on different concentration of DHE (1, 10 and 100 μ M) was also evaluated.

The interference of NPs with the optical detection of DCFH-DA assay was assessed by incubation of different concentrations of NPs with defined amounts of DCFH. DCFH-DA was dissolved in DMSO to a concentration of 10 mM. Before using DCFH-DA in a cell-free system, DA was cleaved off by incubation with NaOH in the dark (NaOH : DCFH-DA = 2 : 1 mol/mol) for 30 min at room temperature. The resulting DCFH was neutralized with 25 mM phosphate buffer (NaH₂PO₄: Na₂HPO₄ = 1:1 v/v; pH 7.4) and the solution was kept in the dark at -20 °C until use. A 10 μ M DCFH was then added to the wells of a 96-well plate loaded with defined amount of NPs and fluorescence was measured over 1 h with an excitation and an emission at 485 and 520 nm, respectively. Each experiment was repeated at least three times with five replications. The effect of NPs on different concentrations of

DCFH (1, 10 and 100 μM) was also evaluated. Each experiment was repeated at least three times with five replications.

Additional experiments were performed in the presence of 6-hydroxy-2,5,7,8-tetramethylchroman-2-carboxylic acid (Trolox) to determine if the change in fluorescence signal observed with NPs was only due to the optical interferences of NPs, or if they interfered with DCFH oxidation. Trolox, a water-soluble vitamin E analogue, is a free radical scavenger and inhibitor of lipid peroxidation. It is able to convert nonfluorescent DCFH to fluorescent DCF.³⁷ Trolox (10 μM) was applied to the plates before, after or during incubation of NPs with DCFH (10 μM). This concentration is known to be sufficient to oxidize DCFH increasing its fluorescence signal.³⁷

To test the effects of NPs on MBCl assay, the following protocols were used. Reaction mixtures containing 20 μM MBCl and different concentrations of NPs in CCM were applied to the plates and compared to wells loaded with MBCl or NPs alone in terms of fluorescence. The effect of NPs on different concentration of MBCl (2, 20 and 200 μM) was also evaluated. Fluorescence readings for all of the experiments were done after 15, 30, 45 and 60 min of incubation at 37 °C. Afterwards, the second series of experiments was done in the presence of GSH to determine whether the changes in fluorescence were induced by the interaction between NPs and GSH. For this, 96-well plates were loaded with 20 μM MBCl, 60 μM GSH and different concentrations of NPs in CCM. The mixtures were incubated for 30 min at 37 °C and fluorescence was measured. In the third series of experiments, adsorption of GSH onto the surface of the NPs was tested by incubating GSH (60 μM) with different concentrations of NPs in CCM for 2 h at 37 °C. Then, 20 μM MBCl was added to each well and incubated for another 30 min at 37 °C. For each series of experiments, fluorescence signals were analysed

with excitation and emission wavelengths at 355 and 460 nm, respectively, using the plate reader. Each experiment was repeated at least three times with five replications.

Optimization of *in vitro* protocols in cell system

To determine the applicability of *in vitro* protocols for risk assessment of metallic NPs, two conventional cell viability assays (MTT and CCK-8) were tested using HepG2 cells line. The cells were cultured in DMEM medium, supplemented with 10 % vol. FBS, 20 IU/mL penicillin and 20 µg/mL streptomycin. The cells were seeded at a density of 10^6 cells/mL and maintained at 37 °C in a humidified atmosphere of 5 % CO₂ in air. The medium was replaced every 2-3 days. Upon reaching 80 % adherent confluence, the cells were seeded in 96-well tissue culture plates (3×10^4 cells/100 µL growth medium/well) in DMEM and incubated overnight at 37 °C. Then, the cells were treated with different concentrations of NPs. In each experiment, the stock NP suspensions were sonicated and freshly diluted to appropriate concentrations in the cell medium. Negative controls without treatment were performed for each analysis. DMSO-treated cells were used as positive controls. NPs were added to quintuplicate wells to a final concentration ranging from 0 to 100 mg/L and incubated for another 24 h. At the end of the exposure, the reliability of both assays, WST-8 and DCFH-DA, were evaluated in control and exposed cells. To minimize the NP interferences, reagents were added either directly or after washing of cells with 100 µl PBS/well. One, two and three washing steps were tested. In the WST-8 assay, 10 µL of WST-8 solution was added to each well. After 4 h incubation at 37 °C, the optical density at 450 nm was determined for each well using a VictorTM multiplate reader (Perkin Elmer, MA, USA). In the DCFH-DA assay, experiments were done by incubating the cells with different concentrations of NPs for 1 h at 37 °C. Cells treated with hydrogen peroxide (500 µM H₂O₂) were used as positive controls and non-treated cells were used as negative controls. After treatment, the washing steps with

PBS were introduced followed by staining with 10 μ M DCFH-DA for 30 min at 37 °C. Cells were then washed twice with PBS and analysed using a plate reader at an excitation wavelength of 485 nm and emission wavelength of 535 nm. Data are expressed as percentage fluorescence compared with relevant negative controls.

Statistical analysis

Data represent mean and standard deviations (SD). Differences between treatments for the different measured variables were tested using simple and repeated measures ANOVA, followed by Fisher LSD posthoc test when significant differences were found ($p < 0.05$). The homogeneity of variances was tested using the Levene test. The level of significance ($p < 0.05$) is indicated by the asterisks. When most data were significantly different compared to relevant controls, only non-significant differences were indicated with the letter n. All statistical analyses were carried out using STATISTICA v12.0 software (StatSoft, Inc., Tulsa, USA).

Results and discussion

In order to predict the biocompatibility and safety of various nanoproducts, one needs to establish *in vitro* toxicity tests that can be used to screen nanomaterials. The establishment and standardization of protocols for NP *in vitro* testing implies a good understanding of the assay and possible interaction of NPs with assay system with respect to the parameters measured.⁷⁻¹⁰ In this study, six conventional *in vitro* assays were compared in terms of their validity to assess toxicity and biocompatibility of well-characterized silver and maghemite NPs stabilized with different surface coatings. Evaluation was performed following the experimental scheme presented in Figure 1.

Characterization and stability evaluation of AgNPs and γ -Fe₂O₃NPs

Nanoscale size, large surface area and unique material properties compared to micro-sized counterparts are the main characteristics of NPs. In addition, metallic NPs have to be coated with various types of polymers and surfactants to improve their biocompatibility and colloidal stability in aqueous media, i.e. to prevent their agglomeration.³⁸ Depending on their characteristics, NPs will either diffuse or aggregate within certain media.⁸ The colloidal stability of metallic NPs *in vitro* depends on the pH, ionic strength, concentration of the biomolecules and redox conditions of the media.³⁹

Generally, *in vitro* examinations require dispersing NPs into the culture medium. The cell culture medium contains several inorganic salts, proteins, amino acids, and vitamins as cell nutrients, which may affect NP stability. Although numerous *in vitro* nanotoxicity studies have already been published, inconsistencies in results from the same type of NPs are frequently reported. Determination of NP colloidal stability, especially under biologically relevant conditions, is typically beyond the scope of toxicological studies. Poor NP characterization and unknown stability during *in vitro* testing may lead to various artifacts.²² A thorough characterization and stability evaluation of NPs are thus critical to robustly interpret the results of *in vitro* testings and understand their behaviour in biological media.^{9,14,22,23}

While the *in vitro* or *in vivo* effects of different NPs characteristics, such as size and chemical composition, on biocompatibility and toxicity have been published in many different papers, the correlation between surface coating and behaviour of NPs in biological media is still a question that needs to be resolved. Therefore, we prepared AgNPs and γ -Fe₂O₃NPs of similar sizes but stabilized with different surface coatings. This study began with an evaluation of the physicochemical properties of the NP dispersions under experimentally relevant conditions.

As the first step, changes in particle size, surface charge and aggregation behaviour of purified NPs were carefully examined in both UPW and CCM using TEM, DLS and ELS. Table 2 summarizes data obtained for hydrodynamic diameter (d_H), polydispersity index (PDI) and ζ potential values. DLS measurements of AgNPs in UPW showed that the volume size distribution was bimodal for all AgNPs except for AOTAgNP and CTAAGNPs characterized by monomodal and trimodal distribution, respectively. In terms of size, almost all AgNPs were in the range from 4.7 to 19.9 nm (Table 2). Only BrijAgNPs were larger with peak maximum at 69.2 ± 6.7 nm (66 %) and 227.1 ± 13.8 nm (34 %). Recorded TEM micrographs were in accordance with DLS data. All of the AgNPs visualized by the TEM were spherically shaped except rod-like CITAgNPs (Figure 2). All AgNPs were well-dispersed in UPW with the exception of CTAAGNPs, which formed aggregates (Figure 2). The UV-Vis absorption spectra presented in Figure S1, given in Supporting Information (SI), also proved the formation of metallic NPs and were in accordance with both the DLS and TEM data. For all AgNPs, the position of the surface plasmon resonance (SPR) peaks was between 380 and 430 nm. The broadened peaks of TweenAgNPs, CTAAGNPs and CITAgNPs can be easily explained with the higher polydispersity of these NPs dispersions (PDI value of ~ 0.5). Table 2 also shows that all AgNPs, except PLLAgNPs and CTAAGNPs, have negative ζ potential ranging from -9.4 ± 1.3 mV (TweenAgNPs) to -39.9 ± 0.1 mV (CITAgNPs). Also, all three investigated types of γ -Fe₂O₃NPs had negative ζ potentials. For UN γ -Fe₂O₃NPs and MAN γ -Fe₂O₃NPs, the monomodal size distributions were observed using DLS (Table 2), while the ζ potentials values of -30.6 ± 1.0 and -26.9 ± 1.1 mV, respectively, indicated good colloidal stability of these particles in UPW. Although PLL coating should have led to the net positive surface charge, the ζ potential of PLL γ -Fe₂O₃NPs close to zero (-5.4 ± 1.0 mV) could be the result of negative ions left after synthesis and attached to the PLL. The same effect was observed for PVPAgNPs and TweenAgNPs bearing an overall negative charge of -11.2 ± 2.3

and -9.4 ± 1.3 mV, respectively. Both coating, PVP and Tween 20, are neutral molecules and should lead to a net surface charge close to zero. Obviously, BH_4^- anions left after synthesis and attached to the surface coatings of PVPAgNPs and TweenAgNPs leading to slightly negative ζ potentials. Having in mind the results of ELS, the considerable proportion (68 %) of larger *i.e.* aggregated, particles found for PLL γ -Fe₂O₃NPs is comprehensible. The ζ potential is based on the mobility of a particle in an electric field. It is related to the electrical potential at the junction between the diffuse ion layer surrounding the particle and the bulk solution.⁴⁰ The ζ potential is related to both surface charge and the local environment of the particle giving indication of colloidal stability. The high ζ potential, either negative or positive, indicates high NP stability because it provides a repulsive force keeping the NPs away from each other *i.e.* NPs tend to repel each other and exhibit no tendency for aggregation. However, when the ζ potential approaches zero, interparticle repulsion decreases as well as the stability of the dispersion, resulting in a weak reversible flocculation.⁴⁰ As expected, all NPs with ζ potential <20 mV or > -20 mV were characterized with bi- or trimodal size distributions with a certain proportion of larger particles (aggregates).

Furthermore, the influence of coating type on AgNPs or γ -Fe₂O₃NP stability in biological environment was evaluated upon dispersing in cell-free culture medium (CCM). In agreement with previous studies,^{23,41} higher ionic strength of medium caused a significant aggregation of all NPs, except for PVPAgNPs, while TweenAgNPs and PLL γ -Fe₂O₃NPs aggregated only slightly. From the colloidal chemistry point of view, CCM is a complex medium, where different interactions at the nanoscale level could be expected. A stable NP dispersion requires a dominant electrostatic or steric repulsive force to maintain the particles separated. NP stability is affected if the attractive forces dominate, or particle collision is energetically favored.³⁵ It is clear that the additives present in CCM decreased the stability of metallic NPs

by decreasing the absolute value of ζ potential values for the tested NPs (Table 2). Upon dispersing the tested NPs in the CCM, the electrostatic stabilization was not sufficient to prevent aggregation or agglomeration which can be seen from the measured d_H values (Table 2). Surface charge became more negative only for TweenAgNPs, PVPAgNPs and PLL γ -Fe₂O₃ NPs which did not show significant differences in the size distributions between UPW and CCM. The TEM micrographs were in accordance with DLS measurements showing particles organized in agglomerates, which were in nano- or micrometers (SI, Fig. S2).

These findings have important implications for interpretation of possible interferences with *in vitro* assays. Change in characteristics and stability of NPs may alter their potential interactions with components of the assays as well as optical measurements performed during the running of *in vitro* assays. Additionally, the aggregation behaviour of certain types of NPs may lead to wrong interpretations of the exposure dose applied during *in vitro* testing. When a colloiddally unstable NPs dispersion is applied to cells, the cell exposure concentration will differ by the large aggregated NPs compared to individual NPs.^{24,42,43}

Interferences of AgNPs and γ -Fe₂O₃NPs with cell viability assays in cell-free system

Various cellular processes determine cell viability, which is the most commonly investigated parameter in cytotoxicity testing. Detection of mitochondrial activity, as one of endpoints used to evaluate cell viability, can be assessed using assays based on spectrophotometrical determination of the reduction of different tetrazolium dyes in mitochondria of intact cells. In several recent papers, it has been shown that different types of NPs may interact with the substrate, depleting free tetrazolium salt and causing false negative results.⁸ Additionally, NPs may absorb or scatter UV-Vis light which will also induce misleading viability results.^{14,16}

As the first step in the evaluation of effects of surface coating of AgNPs or γ -Fe₂O₃NPs on cell viability tests, MTT, MTS and WST-8 assays were performed in CCM according to the

manufacturer's instruction. We observed important differences in NP interference with cell viability assays depending on the NP metal type, their surface coating, and the assay tested. Results are presented in Figures 3a-c. The MTT assay was the most vulnerable to the presence of NPs. The presence of AgNPs increased absorbance significantly at the MTT-formazan peak wavelength compared to negative control already at the low dose of 5 mg/L (Figure 3a). The γ -Fe₂O₃NPs significantly increased absorbance at a higher concentration than AgNPs (10 mg/L; Figure 3a). For all of the tested NPs, the absorbance increase was dose-dependent, which has already been described in several recent papers for other types of metallic NPs.¹⁴⁻¹⁸ The optical properties of NPs, like surface plasmon resonance and quantum confinement, may be the main reason for observed interferences during optical readouts of cell viability assays. Thus, the absorbance of NPs alone was determined at the wavelengths used for the MTT, MTS and WST-8 assays, i.e. 590, 490 and 450 nm, respectively. All of the tested NPs absorb at these wavelengths which is also obvious from their UV-Vis absorption spectra (SI, Figure S1). However, the results showed that a significant absorbance increase compared to the tetrazolium salt (TS) controls started at the NP concentration of 50 mg/L. The lowest increase in optical readouts was induced by AOTAgNPs, BrijAgNPs and TweenAgNPs. Interestingly, the extent of interferences of these three AgNP types was low for MTS and WST-8 assays, but comparably high for the MTT assay just like any other AgNP.

An enhancement of light absorption at the MTT-formazan wavelength by NPs therefore gave false positive results leading to an underestimation of NP toxicity. In order to avoid these shortcomings, background absorbance was subtracted on a plate reader. However, subtraction did not remove high absorbance at the formazan peak for all NPs concentrations (Figures 3a-c). Suspensions above 50 mg/L had significantly higher absorbances at 590, 490 and 450 nm compared to TS controls. This means that the optical properties of NPs were not the main reason for observed interferences with cell viability assays. Although necessary, determining

background NP signals in cell-free viability controls is not sufficient to avoid false results. Thus, other modes of interferences were inspected, like reaction with or binding of assay components. Although it is unlikely that formazan would be formed from MTT in the absence of cells, the obtained data revealed an increase in absorbance with an increase in NP concentration even after the subtraction of NP background absorbance. Figure 3a clearly shows that all AgNPs produced MTT-formazan already at > 5 mg/L. The effect was higher for neutral and positively charged AgNPs compared to negatively charged CITAgNPs and AOTAgNPs. The possible explanation could be a stronger interaction of negatively charged tetrazolium dye with neutral and positively charged AgNPs. The γ -Fe₂O₃NPs induced the lowest increase in absorbance at 590 nm, even lower than negatively charged AgNPs (Figure 3a). Unlike AgNPs, formazan production by γ -Fe₂O₃NPs was more pronounced in the MTS and WST-8 assays compared to the MTT assay. It is also interesting to note that for MTS and WST-8 assays at NPs concentrations > 10 mg/L, subtraction of NPs background signal not only annulled increased absorbance caused by the presence of NPs, but decreased optical readouts by more than 20 % (Figures 3b-c). The reason could be the electrostatic interaction of metallic NPs with MTS-formazan or WST-8-formazan leading to shifts in the UV-Vis spectra and decrease in absorption at 490 or 450 nm. This is in accordance with other studies where the interference with formazan was attributed not only to the light-adsorbing properties of NPs, but also to the adsorption of different formazan products to NP detection.^{17,18,25,26}

To compare the adsorption of MTT and WST-8 or their formazan products on the NPs, a centrifugation step was introduced in the protocols after an incubation period of 4 h. In the MTT assay, samples were centrifuged after the formazan solubilisation step, i.e. addition of DMSO. Centrifugation may be useful to solve interference problems if the NPs do not adsorb assay dyes, thus preventing their measurement. Figure 4a clearly shows that centrifugation was effective in reducing optical signals. However, it also shows that the adsorption of both

types of formazan products to NPs surface occurred. The adsorption of WST-8-formazan was higher by > 40% compared to MTT-formazan solubilized in DMSO for both types of metallic NPs. This is opposite with results published for carbon nanotubes.^{25,26} Concerning the more hydrophilic character of AgNPs and γ -Fe₂O₃NPs compared to carbon nanotubes, the addition of DMSO may destabilize their binding with MTT-formazan. In both MTT and WST-8 assays, there were no clear concentration-dependent adsorptions of formazan to NPs (Figure 4a). Although other studies showed no interference of other metallic NPs (TiO₂, SiO₂, MgO and ZnO) with the WST assay,^{5,27} our results clearly presented the ability of AgNPs and γ -Fe₂O₃NPs to interact with water-soluble WST dye.

In order to differentiate the adsorption of tetrazolium salt to NPs from the adsorption of formazan to NPs, the incubation of NPs with tetrazolium reagent reduced to formazan with ascorbic acid (AsA) was tested. The controls were tetrazolium salt and formazan generated by AsA in the absence of NPs. The formazan concentration was measured before and after centrifugation. For MTT assay, almost all of the tested NPs caused a reduction in the measured formazan before centrifugation (Figure 4b). This reduction was less pronounced with an increase in NP concentration. This indicates that a certain amount of MTT was bound to NPs and disabled to be oxidized by the AsA, but simultaneously, MTT was oxidized to formazan at higher NP concentrations. Only PVPAgNPs did not significantly affect the amount of generated formazan. This is consistent with a previous experiment which also showed that PVPAgNPs did not adsorb the MTT reagent (Figure 4a). Another plausible explanation may be that the adsorption of MTT onto NP surfaces occurs concurrently and concomitantly with its oxidation by the same NPs. It is also possible that DMSO is more effective at reversing formazan binding NP during the MTT assay. After centrifugation, a significant decrease in measured formazan was observed for all NP types and for both MTT

and WST-8 assays in a dose-dependent manner (Figures 4b-c). This is a strong proof of formazan binding to NPs. The PLLAgNPs exhibited the strongest adsorption capacity.

All of the tested particles exhibited evidence of physicochemical interactions with cell viability assay compounds. Neutral and positively charged AgNPs were the most effective in converting tetrazolium compounds and producing formazan under cell-free conditions at ≥ 5 mg/L. The γ -Fe₂O₃NPs have also been found to reduce TSs to formazan under cell-free conditions, but at 10 times higher concentrations. The results presented in Figure 4a-c proved that AgNPs and γ -Fe₂O₃NPs were efficient in adsorbing both the TSs and formazan products at concentrations ranging 1-50 mg/L. Thus, the cell viability assays would be only valid for toxicity assessment of NPs at concentrations that do not reduce TSs or do not adsorb assay reagents or products. There is an obvious need to consistently apply the protocol adaptations using several lines of control experiments. Although we demonstrated that control experiments including the optical readout of assay components and NPs alone help to overcome the interference of cell-associated γ -Fe₃O₄ NPs and to avoid false negative results, our results on AgNPs imply that such adaptations may not be sufficient to make cell viability assays applicable and feasible for evaluation of wide range of metallic NPs. The centrifugation step to remove NPs from the wells, already proposed procedures to overcome these interferences,^{5,27} can even lead to further shortcomings during *in vitro* analysis. Extra washing steps before TS addition may be simple, efficient and promising solution. However, NPs easily stick to cells or container walls even after rinsing. The effectiveness of the rinsing also depends on the particle surface characteristics. This complicates the adaptation of protocols for avoiding interferences. Cell viability assays are dependent on live cells that convert TSs in their metabolic pathways. It is difficult to design a perfect and accurate control during experiments to reproduce what happens to an assay compounds in a cell system. The

ways in which NPs can interfere with the cell viability assay are rather complex and careful validation of results is needed when employing this assay for NP toxicity evaluation.

Interferences of AgNPs and γ -Fe₂O₃NPs with fluorescence probes in cell-free system

Fluorescence probes are widely used for the detection of reactive oxygen species (ROS). ROS formation by redox reactions and oxidant injury are a paradigm of the toxic potential of NPs.³⁰ ROS production is a critical event in toxic effects if the protective mechanisms of cells are overwhelmed causing an oxidative stress.³⁹ Such a state of redox disequilibrium may lead to adverse biological effects like damage to proteins, DNA or lipids resulting in excess cell proliferation, apoptosis, lipid peroxidation, or mutagenesis.³⁹ GSH is a major endogenous antioxidant scavenger and the GSH-mediated antioxidant defence system is critical for protection of cells against oxidative stress. There are many reports that metallic NPs induced oxidative stress by ROS generation, oxidation of biomolecules, and enhancement of antioxidative systems in cells.⁴⁴⁻⁴⁶ It has also been reported that GSH cellular levels are either increased or decreased after *in vitro* treatment with NPs.^{47,48} Therefore, this study tested the impact of different surface coatings of silver and maghemite NPs on their interferences with the three most simple and common methods for the evaluation of oxidative stress response, based on DCFH-DA, DHE and MBCl fluorescent probes. Like in the cell viability assays, a number of NPs also seem to interact directly with fluorescent dyes, thereby compromising their measurement.^{17,28,49}

First, an incubation of each fluorescent probe with NPs was done at different time points (15, 30, 45 and 60 min) to assess fluorescent change with time (Figures 5a-c). Three different concentrations of each fluorescence probe were tested (SI, figure S3). After careful examination, concentrations of 10, 20 and 10 μ M were chosen for DCFH-DA, MBCl and DHE, respectively. Thus, the spontaneous oxidation of all three dyes was followed during 1 h

in the presence of NPs. As NPs may produce background fluorescence in the absence of the probe, changes in fluorescence intensity during 24 h were monitored for each NP alone. Interferences were tested for the NP concentration range 0.1 - 1000 $\mu\text{g/L}$ (Figure 6a-c). Observed background fluorescence was subtracted from the fluorescence of the corresponding reaction mixture. An apparent reduction in fluorescence signal was observed in each assay for almost all of the tested NPs (Figures 5a-c). This suggests that NPs interact with dyes through quenching the fluorescence, which is consistent with previously published data.^{13,14,17,18} For the DCFH assay, a time- and dose-dependent decrease in fluorescence was obtained with all $\gamma\text{-Fe}_2\text{O}_3$ NPs during 60 min, while DCF fluorescence decreased with increased AgNP dose only during the first 45 min (Figure 5a). We observed no clear effect of surface coating of NPs on their ability to quench the DCF fluorescence. However, dextran-coated maghemite NPs was reported to increase DCF fluorescence,¹⁸ while our results showed that uncoated, PLL-coated and *D*-mannose-coated $\gamma\text{-Fe}_2\text{O}_3$ NPs quenched DCF fluorescence (Figure 5a).

Fluorescence quenching is a well-known characteristic of metallic NPs, based on their electrical interactions, which has already been exploited to manipulate the behaviour of fluorophores in their vicinity.⁴⁹ Previous studies reported that metallic NPs could either quench or enhance the fluorescence. According to previous studies reporting fluorescence enhancement by AgNPs⁴⁹ and the fluorescence spectra of tested NPs (SI, Figure S1b), we also expected fluorescence enhancement during testing interferences with DCFH, DHE and MBCl assays. Observed fluorescence quenching may be static and could be ascribed to an association and interaction of the dyes with the NPs. If this is true, a single NP would be able to complex more than a single dye. Bound to the metal surface, very fast energy transfer from the dye to NPs leads to static quenching behaviour. With the increase of NP concentration, the amount of free dyes in solution will decrease and thus, the fluorescence signal will be decreased. This scenario could be ascribed to the interaction of tested NPs with all of the

tested dyes. Quenching of fluorescent dyes by metallic NPs was shown to occur presumably by adsorption onto NP surface.⁴⁹

However, incubation of DHE and MBCl dyes with the tested NPs did not show time-dependent quenching (Figures 5b-c). Moreover, BrijAgNPs did not induce any significant effect, while CTAAgNPs and PLLAgNPs induced fluorescence enhancement in DHE assay after 30 min (Figure 5b). It is likely that CTAAgNPs and PLLAgNPs exhibited increased oxidative potential leading to the massive production of oxidative species during DHE assay which masks fluorescence quenching. All of the other NP types decreased the fluorescence signal which may be additionally explained by the ability of NPs to absorb light in the visible spectrum (see Figure S1a in SI). Since both the excitation and the emission wavelengths of the fluorescent dyes used in this study lie within the visible light spectrum, metallic NPs may absorb not only the emission but also the excitation energy. Another reason for decreased fluorescence could consist in the light scattering of NPs.

Changes in fluorescence intensity were the lowest in the MBCl assay. It should be emphasized that MBCl dye is nonfluorescent until it forms adducts with GSH. As GSH was not added in the experiments from Figures 5a and 6a, the decreased fluorescence signal measured in the presence of NPs resulted from the light scattering of NPs. Therefore, the effect of AgNPs and γ -Fe₂O₃NPs on the reaction between the MBCl probe and GSH was evaluated. It has been shown here that MBCl forms adducts exclusively with GSH,³⁶ which can be fluorometrically measured. After incubating GSH and MBCl with different concentrations of NPs, a significant increase in GSH-MBCl fluorescence was observed after 30 min for NP concentrations > 10 mg/L (Figure 7a). The observed enhancement may be due to resonance energy transfer and electric field interaction described by Mie's theory of scattering. Higher NP concentrations caused a depletion of GSH-MBCl fluorescence signal probably due to the adsorption of S-containing GSH onto the NP surface which was then no

longer available for the formation of a GSH-MBCl adduct. Dramatic fluorescence signal decrease was observed after 24 h of incubation with NPs, while GSH-MBCl fluorescence was stable during 24 h. For both time points, fluorescence changes were dose-dependent; being lower with higher NP concentrations applied (Figure 7a). The highest decrease was observed for PLLAgNPs, CTAAgNPs and PVPAgNPs indicating their enhanced adsorption ability. In the next experiment, GSH was first incubated with NPs for 2 h. The MBCl probe was then added and fluorescence signal measured after 35 min of incubation. The results showed that a dose-dependent decrease of fluorescence intensities occurred already at an NP concentration of 1 mg/L (Figure 7b). The interaction with GSH was the most pronounced for positively charged AgNPs and γ -Fe₂O₃NPs. Without adapting the MBCl assay, NP interferences would lead to false lower GSH values. The question remains if this problem can be overcome. Any treatment with metallic NPs would lead to adsorption of GSH from the cell or tissue culture onto NPs surface. Removing NPs by washing or centrifugation prior to the application of the MBCl dye would also remove the adsorbed GSH. A possible way out is to work within the NP concentration range, which would not significantly influence GSH level.

To determine the effects of AgNPs and γ -Fe₂O₃NPs on the oxidation reaction of DCFH to DCF, a Trolox antioxidant was used in the last series of experiments with fluorescent probes. The incubation of Trolox with DCFH is known to result in a time- and dose-dependent increase in DCF fluorescence.³⁷ During incubation, the abstraction of hydrogen from DCFH to the Trolox phenoxyl radical resulted in the formation of fluorescent DCF. Upon addition of AgNPs or γ -Fe₂O₃NPs in incubation medium of DCFH and Trolox, DCF fluorescence quenching was observed only for neutral and negatively charged AgNPs, while γ -Fe₂O₃NPs and positively charged AgNPs caused an enhancement of the fluorescence signal (Figure 8a). Next, DCFH-DA was incubated first with NPs for 24 h when Trolox was added to the reaction mixture. The resulting fluorescence intensity was significantly increased in a dose-

dependent manner compared to control (DCFH + Trolox). A higher dose of γ -Fe₂O₃NPs and positively charged AgNPs produced a higher DCF fluorescence (Figure 8b). Although fluorescence significantly increased with neutral and negatively charged AgNPs, these intensities decreased with increasing concentrations of NPs. The reason may be that the interaction of NPs with DCFH-DA during incubation produced either DCF or a significant amount of reactive oxygen which could have enhanced the dehydrogenation of Trolox to its phenoxyl radical and subsequently led to significant DCF production. For neutral and negatively charged AgNPs, decreased fluorescence with increasing NP concentration may be the result of competition between NP effect on DCF production and NP light scattering which decreases fluorescence signals as NP concentration increases. The net fluorescence would then be decreased with higher NP concentration. When Trolox was incubated first with NPs for 24 h before addition of DCFH, DCF fluorescence was completely diminished (Figure 8b) indicating the ability of NPs to destroy the Trolox phenoxyl radical.

Our results clearly indicate that fluorescence assays, without prior adaptation, would lead to false-negative results and an underestimation of NP toxicity. Removing NPs from the solution by washing or centrifugation, or lowering NP concentrations to non-interfering levels are possible solutions to avoid methodological artefacts. Apart from this, the control testing of the oxidative potential of each NP type should be performed to find an appropriate incubation time.

Optimization of *in vitro* protocols in cell system

Taking into account the results presented in previous sections, we tested the simplest adaptation strategy for removing NP interferences from the two most common cytotoxicity tests – WST-8 and DCFH-DA assays. We evaluated the efficiency of introducing washing steps during investigation of effects of different AgNPs on cell viability and oxidative stress

response in HepG2 cells. In general, NPs should be eliminated from analysis as much as possible in order to reduce the risk of interferences, e.g. by extensive washing, ultracentrifugation, transferring supernatants, concentration control or other types of method modifications.

Cells were exposed to AOTAgNPs, PVPAgNPs, PLLAgNPs and CTAAgNPs (for details, see Materials and methods). Before the addition of assay reagents, cells were washed 1-3 times with PBS pH 7.4 to remove NPs from wells.

The results presented in Figure 9 are rather indicative. Using only one washing step did not yield accurate results either in the WST-8 or in the DCFH-DA assay. It is clearly visible that the presence of NPs underestimated their cytotoxic effect on HepG2 cells. After 1-2 washing steps, high cell viability (Figure 9a) and decreased ROS level (Figure 9b) were observed. Only the third washing of cells from NPs traces resulted in more reasonable results, which showed the cytotoxic potential of AgNPs depending on surface coating. Positively charged AgNP decreased cell viability at a lower exposure concentration and induced production of higher ROS levels than neutral and positively charged AgNPs. However, the extra washing steps introduced in the protocol may present an additional source of shortcomings. Also, positive and negative controls are necessary to indicate variability, repeatability, accuracy and precision of experiment. The cells can be detached from the culture plate and removed with the supernatants. Therefore, the rinsing protocol should be gentle, careful and highly reproducible. HepG2 cells used in this study are highly adherent and easy to use. The problem may arise with non-adherent cells, like stem cells, and that is when alternative changes to the assay protocol should be considered.

Conclusions

This study compared interferences in six conventional cytotoxicity assays caused by silver and maghemite nanoparticles stabilized with different coating agents. The obtained data demonstrate that *in vitro* evaluations of metallic NPs are not superficial and may result in false conclusions. Table 3 summarizes the type of interferences of each NP with each of the tested *in vitro* assays. For all of the NPs, interferences derived from the optical properties of NPs, their adsorptive capacity and ability for chemical interaction with assay components. Results fluctuated depending on metal core and surface coating of NPs, as well as on the assay system. The observed non-biological artefacts claim that a comprehensive characterization of the intrinsic properties of metallic NPs and their stability in biological media should be performed prior to any biological experiments. Indeed, all of the tested NPs exhibited size distributions that rapidly increased upon suspension in cell culture media implying their instability.

The following recommendations should be adopted in future biomedical evaluations of metallic NPs:

- the tendency of NPs to aggregate in the cell culture media should be examined and used for corrections in experimental design;
- the impact of different NP types, different media, additives and assay compounds should be accounted for and the choice of optimal assay should be based upon the nature of NP interactions with assay components;
- the NP concentration should be decreased as much as possible or even limited in the final sample in order to reduce the risk of interferences, e.g. by extensive washing, ultracentrifugation, transferring supernatants or adaptation of assay;
- as many as possible control experiments should be included during evaluation and multiple assays should be performed, if possible, depending on NP type;

- visual examination of cell cultures after their exposure to NPs may also be critical during investigation.

In view of existing gaps for a robust biomedical testing of novel NPs, it is imperative that any investigation of biocompatibility and safety of NPs be carefully accomplished bearing in mind every possible interference and interaction with the test system.

Associated content

Supporting Information

The protocols for synthesis of silver nanoparticles, UV-Vis and fluorescence spectra of silver nanoparticles, additional data on interferences of tested nanoparticles on DCFH-DA, DHE and MBCl assays.

Author information

Corresponding Author

*E-mail: ivinkovic@imi.hr

Funding

This work was supported by the GlowBrain project (FP7-REGPOT-2012-CT2012-316120; European Commission).

Notes

The authors declare no competing financial interest.

Abbreviations

γ -Fe₂O₃NPs, maghemite nanoparticles; AgNPs, silver nanoparticles; AOTAgNP, sodium bis(2-ethylhexyl)-sulfosuccinate coated silver nanoparticles; AsA, ascorbic acid; BrijAgNP, Brij 35 coated silver nanoparticles; CCM, cell-free culture medium; CITAgNP, trisodium citrate coated silver nanoparticles; CTAAgNP, cetyl trimethylammonium bromide coated silver nanoparticles; DCF, 2',7'-dichlorofluorescein; DCFH, 2',7'-dichlorofluorescein; DCFH-DA, 2',7'-dichlorofluorescein-diacetate; DHE, dihydroethidium; DLS, dynamic light scattering; DMEM, phenol red-free Dulbecco's modified Eagle's medium; DMSO, dimethyl sulfoxide; E, ethidium; ELS, electrophoretic light scattering; EOH, 2-hydroethidium; FBS, fetal bovine serum; GSH, glutathione; HepG2, human hepatoma cells; ICPMS, inductively coupled plasma mass spectrometer; MAN γ -Fe₂O₃NPs, *D*-mannose coated γ -Fe₂O₃ nanoparticles; MBCl, monochlorobimane; MTS, (3-(4,5-dimethylthiazol-2-yl)-5-(3-carboxymethoxyphenyl)-2-(4-sulfophenyl)-2H-tetrazolium); MTT, (3-(4,5-dimethylthiazol-2-yl)-2,5-diphenyltetrazoliumbromide); NPs, nanoparticles; PBS, phosphate buffer solution; PLL γ -Fe₂O₃NPs, poly-*L*-lysine coated γ -Fe₂O₃-nanoparticles; PLLAgNP, poly-*L*-lysine coated silver nanoparticles; PVPAgNP, poly(vinylpyrrolidone) coated silver nanoparticles; ROS, reactive oxygen species; SD, standard deviation; SPR, Surface Plasmon Resonance; TEM, transmission electron microscope; TS, tetrazolium salt; TweenAgNP, Tween 20 coated silver nanoparticles; UN γ -Fe₂O₃NPs, uncoated γ -Fe₂O₃-nanoparticles; UPW, ultrapure water; WST-8, (2-(2-methoxy-4-nitrophenyl)-3-(4-nitrophenyl)-5-(2,4-disulfophenyl)-2H-tetrazolium).

References

1 M. Tang, P. J. Russell and A. Khatri, *Discov. Med.*, 2009, **7**, 68–74.

- 2 S. W. P. Wijnhoven, W. J. G. M. Peijnenburg, C. A. Herberts, W. I. Hagens, A. G. Oomen, E. H. W. Heugens, B. Roszek, J. Bisschops, I. Gosens, D. Van De Meent, S. Dekkers, W. H. De Jong, M. Van Zijverden, A. J. A. M. Sips and R. E. Geertsma, *Nanotoxicology*, 2009, **3**, 109–138.
- 3 B. Nowack, H. F. Krug and M. Height, *Environ. Sci. Technol.*, 2011, **45**, 1177–1183.
- 4 V. V. Mody, R. Siwale, A. Singh and H. R. Mody, *J. Pharm. Bioapplied Sci.*, 2010, **2**, 282–289.
- 5 R. Guadagnini, B. Halamoda Kenzaoui, L. Walker, G. Pojana, Z. Magdolenova, D. Bilanicova, M. Saunders, L. Juillerat-Jeanneret, A. Marcomini, A. Huk, M. Dusinska, L. M. Fjellsbø, F. Marano and S. Boland, *Nanotoxicology*, 2015, **9**, 13–24.
- 6 R. Damoiseaux, S. George, M. Li, S. Pokhrel, Z. Ji, B. France, T. Xia, E. Suarez, R. Rallo, L. Madler, Y. Cohen, E. M. V. Hoek and A. Nel, *Nanoscale*, 2011, **3**, 1345–1360.
- 7 A. Dhawan and V. Sharma, *Anal. Bioanal. Chem.*, 2010, **398**, 589–605.
- 8 A. Kroll, M. H. Pillukat, D. Hahn and J. Schnekenburger, *Eur. J. Pharm. Biopharm.*, 2009, **72**, 370–377.
- 9 V. Stone, H. Johnston and R. P. F. Schins, *Crit. Rev. Toxicol.*, 2009, **39**, 613–626.
- 10 S. A. Love, M. A. Maurer-Jones, J. W. Thompson, Y. S. Lin and C. L. Haynes, *Annu. Rev. Anal. Chem.*, 2012, **5**, 181–205.
- 11 B. J. Marquis, S. A. Love, K. L. Braun and C. L. Haynes, *Analyst*, 2009, **134**, 425–439.
- 12 A. Marucco, F. Catalano, I. Fenoglio, F. Turci, G. Martra and B. Fubini, *Chem. Res. Toxicol.*, 2015, **28**, 87–91.

- 13 M. Rösslein, J. T. Elliott, M. Salit, E. J. Peterson, C. Hirsch, H. F. Krug and P. Wick, *Chem. Res. Toxicol.*, 2015, **28**, 21-30.
- 14 K. J. Ong, T. J. MacCormack, R. J. Clark, J. D. Ede, V. A. Ortega, L. C. Felix, M. K. M. Dang, G. Ma, H. Fenniri, J. G. C. Veinot and G. G. Goss, *PLoS ONE*, 2014, **9**, e90650.
- 15 N. A. Monteiro-Riviere, A. O. Inman and L. W. Zhang, *Toxicol. Appl. Pharm.*, 2009, **234**, 222–235.
- 16 A. L. Holder, R. Goth-Goldstein, D. Lucas and C. P. Koshland, *Chem. Res. Toxicol.*, 2012, **25**, 1885–1892.
- 17 A. Kroll, M. H. Pillukat, D. Hahn and J. Schnekenburger, *Arch. Toxicol.*, 2012, **86**, 1123–1136.
- 18 S. M. Griffiths, N. Singh, G. J. S. Jenkins, P. M. Williams, A. W. Orbaek, A. R. Barron, C. Wright and S. H. Doak, *Anal. Chem.*, 2011, **83**, 3778-3785.
- 19 A. Aranda, L. Sequedo, L. Tolosa, G. Quintas, E. Burello, J. V. Castell and L. Gombau, *Toxicol. in Vitro*, 2013, **27**, 954-963.
- 20 X. Han, R. Gelein, N. Corson, P. Wade-Mercer, J. Jiang, P. Biswas, J. N. Finkelstein, A. Elder and G. Oberdorser, *Toxicology*, 2011, **287**, 99–104.
- 21 T. Pfaller, R. Colognato, I. Nelissen, F. Favilli, E. Casals, D. Ooms, H. Leppens, J. Ponti, R. Stritzinger, V. Puentes, D. Boraschi, A. Duschl and G. J. Oostingh, *Nanotoxicology*, 2010, **4**, 52–72.
- 22 M. Horie, H. Kato, K. Fujita, S. Endoh and H. Iwahashi, *Chem. Res. Toxicol.*, 2012, **25**, 605-619.

- 23 C. Schulze, C. Schulze, A. Kroll, C. Schulze, A. Kroll, C.-M. Lehr, U. F. Schäfer, K. Becker, J. Schnekenburger, C. Schulze Isfort, R. Landsiedel and W. Wohlleben, *Nanotoxicol.*, 2008, **2**, 51-61.
- 24 J. G. Teeguarden, P. M. Hinderliter, G. Orr, B. D. Thrall and J. G. Pounds, *Toxicol. Sci.*, 2007, **95**, 300–312.
- 25 A. Casey, E. Herzog, M. Davoren, F. M. Lyng, H. J. Byrne and G. Chambers, *Carbon*, 2007, **45**, 1425–1432.
- 26 J. M. Wörle-Knirsch, K. Pulskamp and H. F. Krug, *Nano. Lett.*, 2006, **6**, 1261–1268.
- 27 V. Wilhelmi, U. Fischer, D. van Berlo, K. Schulze-Osthoff, R. P. Schins and C. Albrecht, *Toxicol. In Vitro*, 2012, **26**, 323-334.
- 28 S. H. Doak, S. M. Griffiths, B. Manshian, N. Singh, P. M. Williams, A. P. Brown and G. J. Jenkins, *Mutagenesis*, 2009, **24**, 285-293.
- 29 G. Jiao, X. He, X. Li, J. Qiu, H. Xu, N. Zhang, S. Liu, *RSC Adv.*, 2015, **5**, 53240-53244.
- 30 G. J. Oostingh, E. Casals, P. Italiani, R. Colognato, R. Stritzinger, J. Ponti, T. Pfaller, Y. Kohl, D. Ooms, F. Favilli, H. Leppens, D. Lucchesi, F. Rossi, I. Nelissen, H. Thielecke, V. F. Puentes, A. Duschl, D. Boraschi, *Part. Fibre Toxicol.*, 2011, **8**:8.
- 31 S. L. R. Ellison and V. J. Barwick, *Accredit. Qual. Assur.*, 1998, **3**, 101–105.
- 32 D. Horák, M. Babič, P. Jendelová, V. Herynek, M. Trchová, K. Likavčanová, M. Kapcalová, M. Hájek and E. Syková, *J. Magn. Magn. Mater.*, 2009, **321**, 1539–1547.
- 33 D. Horák, M. Babič, P. Jendelová, V. Herynek, M. Trchová, Z. Pientka, E. Pollert, M. Hájek and E. Syková, *Bioconj. Chem.*, 2007, **18**, 635-644.
- 34 M. Babič, D. Horák, M. Trchová, P. Jendelová, K. Glogarová, P. Lesný, V. Herynek, M. Hájek and E. Syková, *Bioconj. Chem.*, 2008, **19**, 740-750.

- 35 J. Chen, S. C. Rogers and M. Kavdia, *Ann. Biomed. Eng.*, 2013, **41**, 327-337.
- 36 H. Kamencic, A. Lyon, P. G. Paterson and B. H. Juurlink, *Anal. Biochem.*, 2000, **286**, 35-37.
- 37 J. F. Kalinich, N. Ramakrishnan and D. E. McClain, *Free Rad. Res.*, 1997, **26**, 37-47.
- 38 A. T. Qureshi, W. T. Monroe, M. J. Lopez, M. E. Janes, V. Dasa, S. Park, A. Amirsadeghi and D. J Hayes, *J. Appl. Polym. Sci.*, 2011, **120**, 3042–3053.
- 39 M. Auffan, J. Rose, M. R. Wiesner and J. Y. Bottero, *Environ. Pollut.*, 2009, **157**, 1127-1133.
- 40 J. A. Fornes, *Colloid. Polym. Sci.*, 1985, **263**, 1004–1007.
- 41 B. F. Leo, S. Chen, Y. Kyo, K.-L. Herpoldt, N. J. Terrill, I. E. Dunlop, D. S. McPhail, M. S. Shaffer, S. Schwander, A. Gow, J. Zhang, K. F. Chung, T. D. Tetley, A. E. Porter and M. P. Ryan, *Environ. Sci. Technol.*, 2013, **47**, 11232–11240.
- 42 S. Elzey and V. H. Grassian, *J. Nanopart. Res.*, 2010, **12**, 1945-1958.
- 43 J. M. Zook, M. D. Halter, D. Cleveland and S. E. Long, *J. Nanopart. Res.*, 2012, **14**, 1165.
- 44 L. K. Limbach, P. Wick, P. Manser, R. N. Grass, A. Bruinink and W. J. Stark, *Environ. Sci. Technol.*, 2007, **41**, 4158–4163.
- 45 T. Xia, M. Kovochich, J. Brant, M. Hotze, J. Sempf, T. Oberley, C. Sioutas, J. I. Yeh, M. R. Wiesner and A. E. Nel, *Nano. Lett.*, 2006, **6**, 1794–1807.
- 46 S. Arora, J. Jain, J. M. Rajwade and K. M. Paknikar, *Toxicol. Lett.*, 2008, **179**, 93–100.
- 47 J. Farkas, P. Christian, J. A. Gallego-Urrea, N. Roos, M. Hasselov, K. E. Tollefsen and K. V. Thomas, *Aquat. Toxicol.*, 2011, **101**, 117–125.
- 48 E. J. Rogers, S. F. Hsieh, N. Organti, D. Schmidt and D. Bello, *Toxicol. In Vitro*, 2008, **22**, 1639–1647.
- 49 C. A. Sabatini, R. V. Pereira and M. H. Gehlen, *J. Fluoresc.*, 2007, **17**, 377–382.

TABLE 1. The *in vitro* assays used in this study.

Assay	Dye/Compound	Type of action detected	Readout
MTT (MTT Cell Proliferation)	(3-(4,5-dimethylthiazolyl-2)-2,5-diphenyltetrazolium bromide (MTT))		Absorbance (590 nm)
MTS (CellTiter 96® AQueous One Solution Cell Proliferation)	3-(4,5-dimethylthiazol-2-yl)-5-(3-carboxymethoxyphenyl)-2-(4-sulfophenyl)-2H-tetrazolium, inner salt (MTS)	Cell viability through determination of mitochondrial function	Absorbance (490 nm)
WST-8 (Cell Counting Kit-8)	2-(2-methoxy-4-nitrophenyl)-3-(4-nitrophenyl)-5-(2,4-disulfophenyl)-2H-tetrazolium, sodium salt (WST-8)		Absorbance (450 nm)
DCFH-DA	2',7'-dichlorofluorescein-diacetate (DCFH-DA)	Production of a variety of reactive oxygen species	Fluorescence; excitation (485 nm) emission (520 nm)
DHE	Dyhydroethidium (DHE)	Production of superoxide radicals	Fluorescence; excitation (485 nm) emission (570 nm)
MBCl	Monochlorobimane (MBCl)	Glutathione level	Fluorescence; excitation (355 nm) emission (460 nm)

TABLE 2. Hydrodynamic diameter (d_H), zeta potential (ζ) and polydispersity index (Pdl) of silver and maghemite nanoparticles with different coatings in ultrapure water (UPW) and cell-free culture medium (CCM) after 1 h.

Particles	UPW			CCM		
	d_H (nm) (% mean volume)	ζ (mV)	PdI	d_H (nm) (% mean volume)	ζ (mV)	PdI
CIT	13.4 ± 2.5 (86%)	-39.9 ± 1.7	0.5	58.7 ± 26.8 (11%)	-19.1 ± 0.9	0.4
AgNPs	63.3 ± 14.1 (14%)			484.4 ± 211.3 (89%)		
AOT	19.9 ± 0.5 (99%)	-27.3 ± 0.1	0.2	35.6 ± 7.6 (7%)	-19.1 ± 1.1	0.3
AgNPs				409.0 ± 74.1 (93%)		
PVP	4.7 ± 0.9 (98%)	-11.2 ± 2.3	0.4	4.1 ± 1.2 (98%)	-6.6 ± 0.6	0.5
AgNPs	33.5 ± 4.0 (2%)			37.9 ± 7.6 (2%)		
Brij	69.2 ± 6.7 (66%)	-36.9 ± 3.2	0.3	52.2 ± 26.3 (17%)	-19.9 ± 2.3	0.3
AgNPs	227.1 ± 13.8 (34%)			269.5 ± 25.6 (83%)		
Tween	5.5 ± 0.3 (98.9%)	-9.4 ± 1.3	0.5	11.3 ± 2.4 (93.2%)	-16.7 ± 1.2	0.6
AgNPs	36.1 ± 2.5 (1.2%)			98.3 ± 15.9 (4.5%)		
PLL	7.4 ± 1.3 (96%)	+23.6 ± 4.0	0.2	18.6 ± 9.5 (4%)	-5.4 ± 2.0	0.3
AgNPs	55.1 ± 13.4 (4%)			686.6 ± 133.8 (96%)		
CTA	6.2 ± 4.6 (70%)	+37.6 ± 1.6	0.5	100.1 ± 51.6 (27%)	-8.3 ± 3.0	0.4
AgNPs	40.0 ± 17.4 (26%)			442.7 ± 175.3 (73%)		
	158.5 ± 62.2 (4%)					
UN	109.15 ± 2.7 (99%)	-30.6 ± 1.0	0.2	765.7 ± 170.4 (99%)	-18.8 ± 0.6	0.4
γ -Fe ₂ O ₃ NPs						
PLL	110.1 ± 15.9 (32%)	-5.4 ± 0.4	0.5	138.8 ± 35.0 (23%)	-14.3 ± 1.1	0.7
γ -Fe ₂ O ₃ NPs	499.8 ± 127.9 (68%)			688.6 ± 167.3 (77%)		

MAN	100.9 ± 3.7 (98%)	-26.9 ± 1.1	0.2	723.0 ± 170.6 (99%)	-17.9 ± 0.7	0.3
γ -Fe ₂ O ₃ NPs						

TABLE 3. Summarized results on interferences of differently coated silver and maghemite nanoparticles with *in vitro* assays.

Assay	NPs type	Interferences	Artefacts	Solutions
MTT and MTS	All AgNPs and γ - Fe_2O_3 NPs >5 mg/L	Optical, production of formazan	Increased cell viability	
		Adsorption of tetrazolium salt or formazan	Decreased cell viability if centrifugation is used	Limiting NPs concentration, background
WST-8	All AgNPs and γ - Fe_2O_3 NPs >10 mg/L	Optical, production of WST-8-formazan	Increased cell viability	subtractions, control
		Adsorption of WST- 8 or WST-8- formazan	Decreased cell viability if centrifugation is used	experiments, extensive washing, avoid
DCFH- DA	All AgNPs and γ - Fe_2O_3 NPs >0.1 mg/L	Fluorescence quenching and adsorption of fluorescent dye	Decreased ROS level	centrifugation, cell counting, flow cytometric analysis
		Positively charged AgNPs and γ - Fe_2O_3 NPs >0.1 mg/L	Oxidation of DCFH to DCF	Increased ROS level
DHE	Neutral and negatively charged AgNPs (except	Fluorescence quenching and	Decreased ROS level	

	BrijAgNPs) and γ - $\text{Fe}_2\text{O}_3\text{NPs} > 0.1 \text{ mg/L}$	adsorption fluorescent dye	of
MBCI	Positively negatively charged AgNPs and $\gamma\text{-Fe}_2\text{O}_3\text{NPs}$ >0.1 mg/L	and Fluorescence quenching adsorption fluorescent dye	and Decreased of GSH level
	All AgNPs and γ - $\text{Fe}_2\text{O}_3\text{NPs} > 5 \text{ mg/L}$	Adsorption of GSH	Decreased GSH level

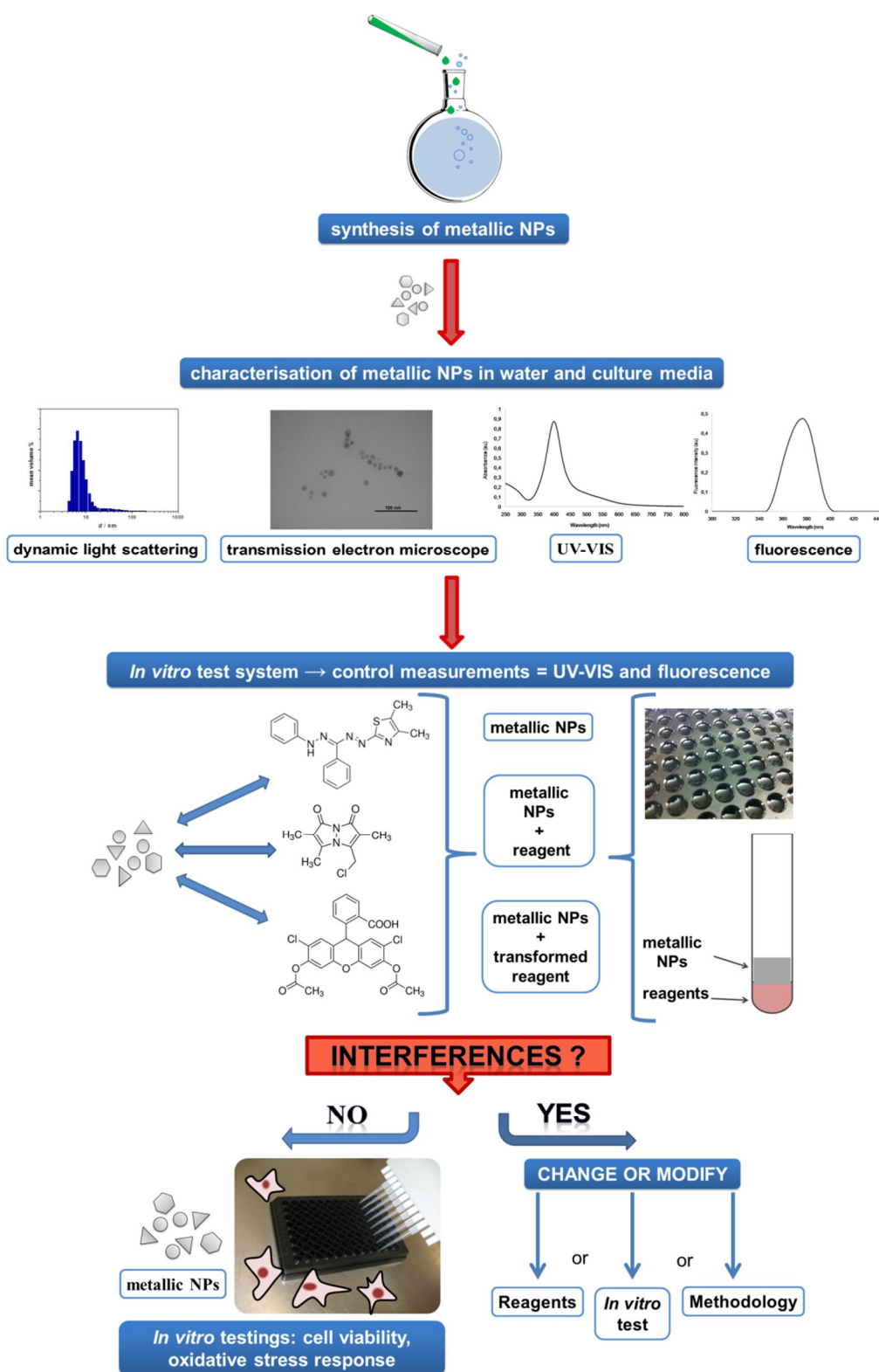


Figure 1. Experimental setup for *in vitro* evaluation of metallic nanoparticles.

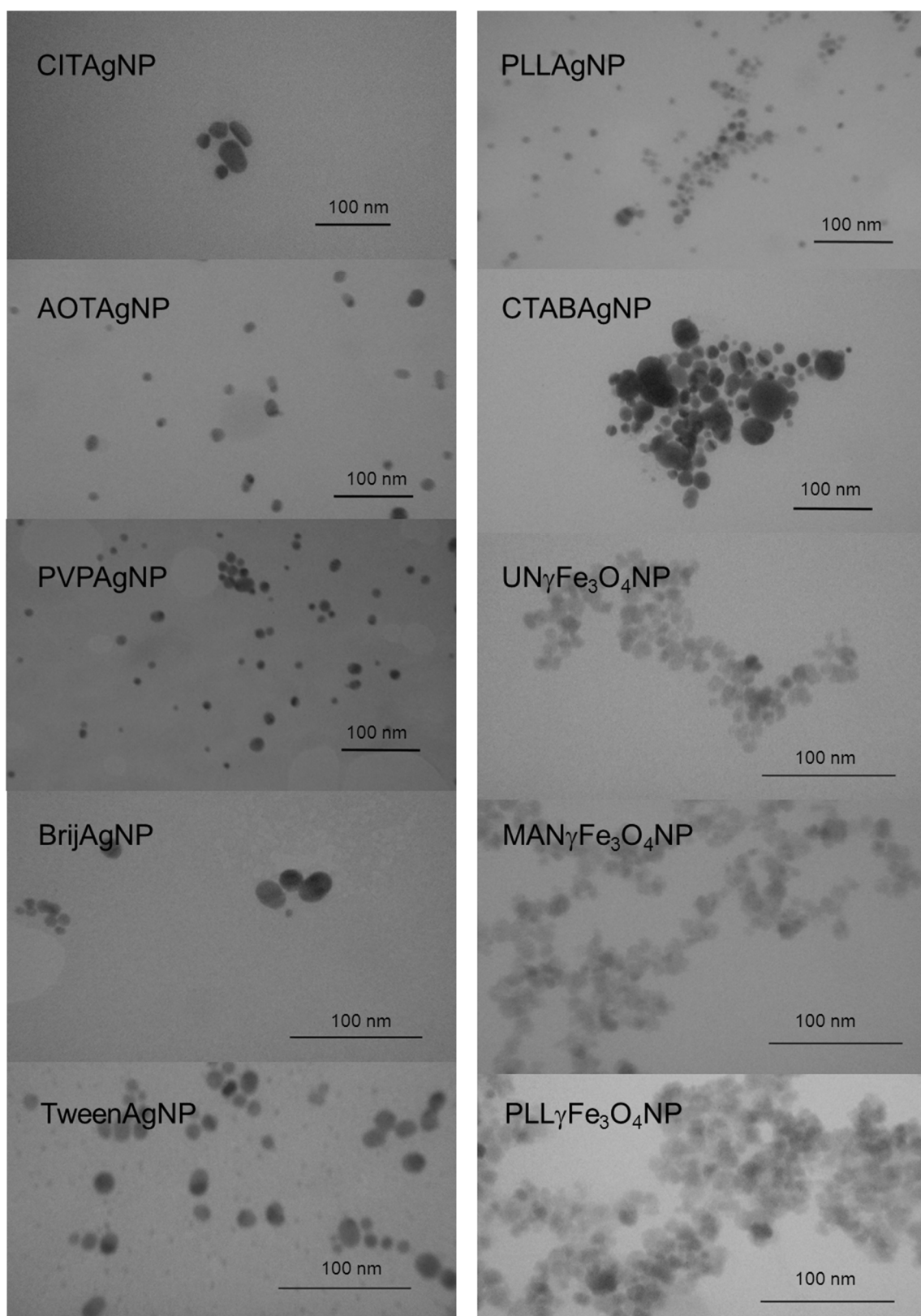


Figure 2. Transmission electron micrographs (TEM) of silver nanoparticles coated with trisodium citrate (CITAgNP), sodium bis(2-ethylhexyl)-sulfosuccinate (AOTAgNP), cetyl trimethylammonium bromide (CTABAgNP), poly(vinylpyrrolidone) (PVPAgNP), poly-*L*-

lysine (PLLAgNP), Brij 35 (BrijAgNP) and Tween 20 (TweenAgNP), and maghemite NPs, uncoated γ -Fe₂O₃-NPs (UN γ -Fe₂O₃NPs), and coated with *D*-mannose (MAN γ -Fe₂O₃NPs) and poly-*L*-lysine (PLL γ -Fe₂O₃NPs).

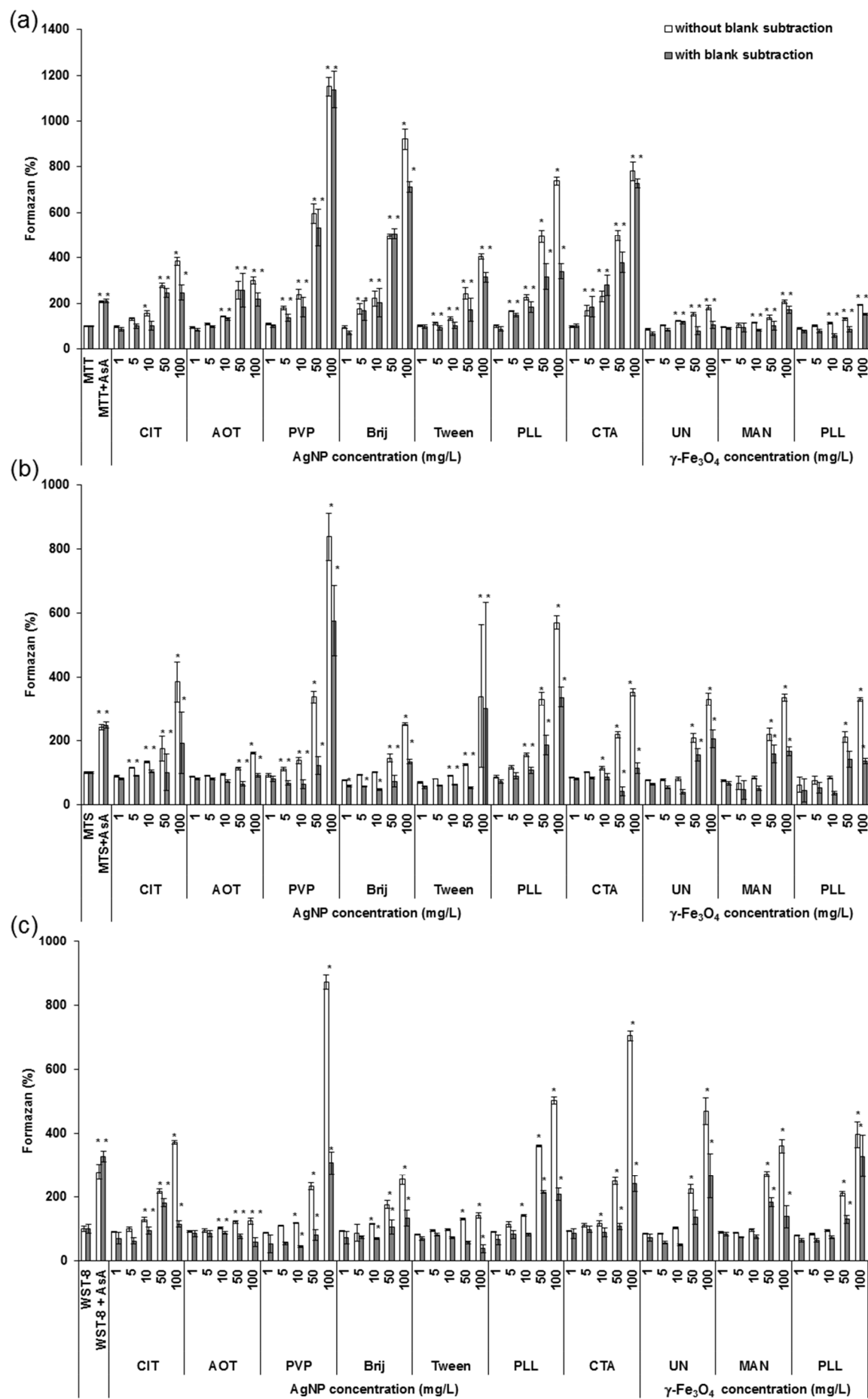


Figure 3. Interferences of differently coated AgNPs and γ -Fe₂O₃NPs with (a) MTT, (b) MTS, and (c) WST-8 cell viability assays. Absorbance of reaction mixture of tetrazolium salts and NPs were presented before (white columns) and after (dark grey columns) background subtraction of control reagents and NPs alone. * indicates significantly different values from the control (tetrazolium salts: MTT, MTS or WST-8) at $P < 0.05$.

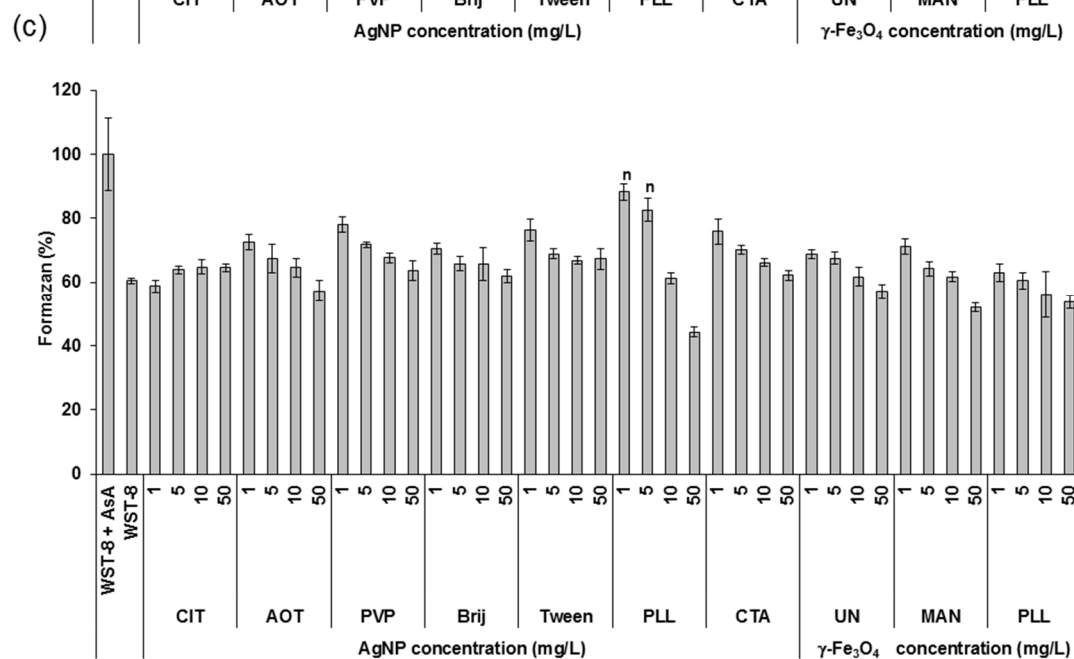
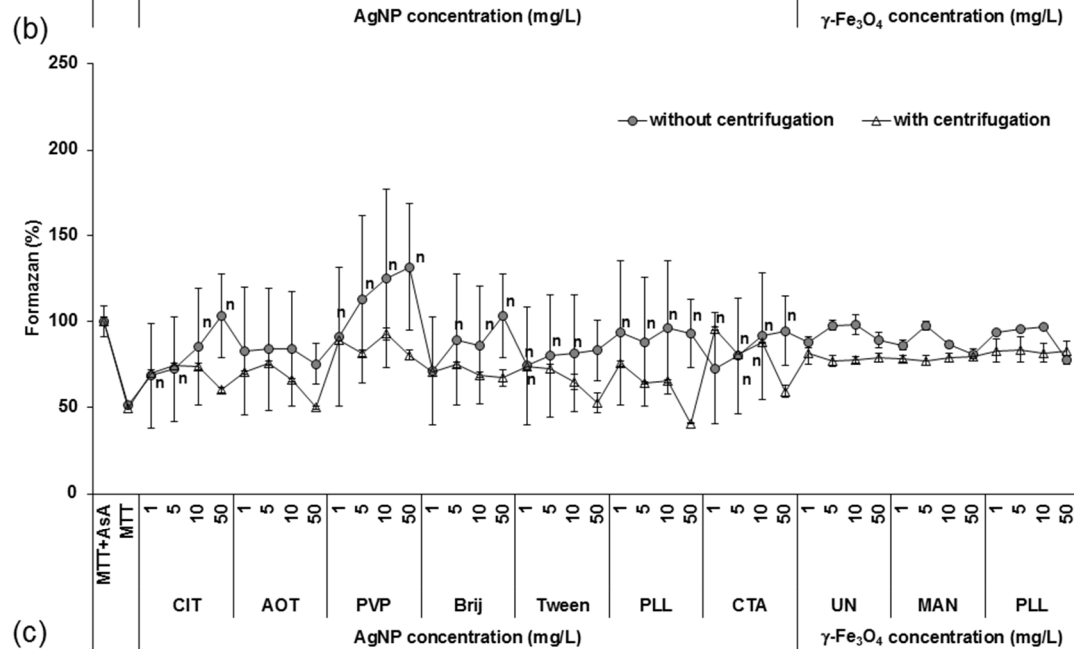
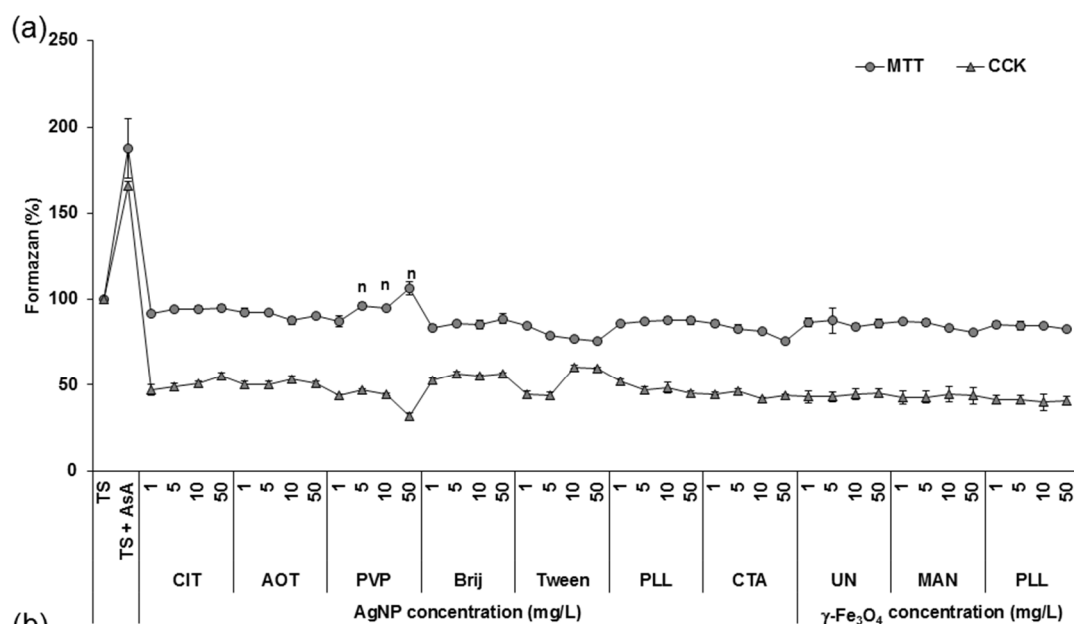


Figure 4. Interferences of differently coated AgNPs and γ -Fe₂O₃NPs with MTT and WST-8 cell viability assays. (a) Absorbance of reaction mixture of NPs and MTT (grey circle) or WST-8 (grey triangle) after centrifugation. (b) Absorbance of reaction mixture of MTT, ascorbic acid (AsA) and NPs before (grey circle) and after (white triangle) centrifugation. (c) Absorbance of reaction mixture of WST-8, AsA and NPs and after centrifugation. ⁿ indicates values that were not significantly different from the control (reaction mixture of NPs, AsA and MTT or WST-8), while all other values were significantly different from the control at $P < 0.05$.

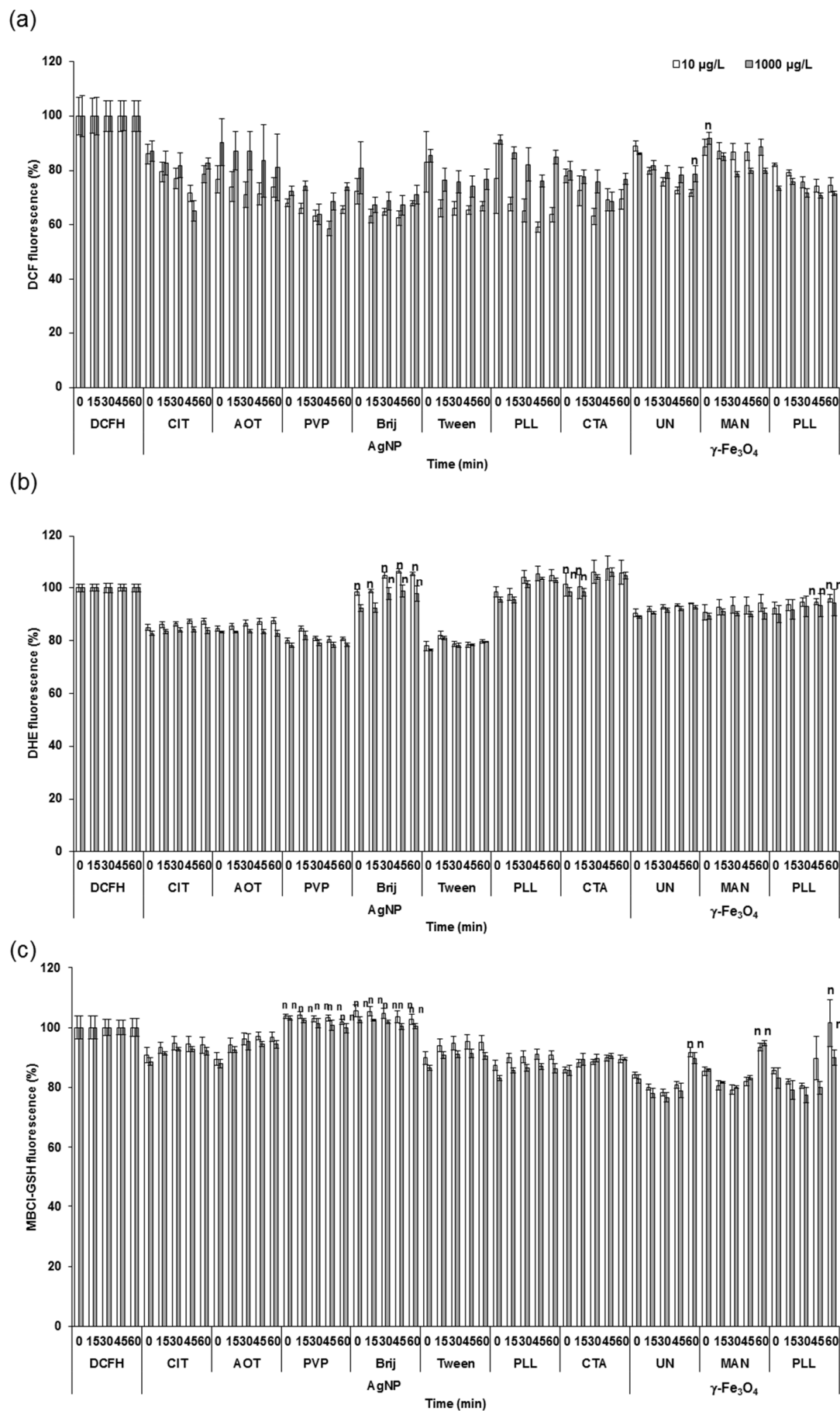


Figure 5. Interferences of differently coated AgNPs and γ -Fe₂O₃NPs with DCFH-DA (a), DHE (b) and MBCl (c) assays at two different NPs concentrations (white columns for 10 μ g/L, and dark grey columns for 1000 μ g/L). Fluorescence was measured at 0, 15, 30, 45 and 60 min after mixing NPs with fluorescent probes in cell-culture media. ⁿ indicates values that were not significantly different from the control (fluorescent probes alone), while all other values were significantly different from the control at $P < 0.05$.

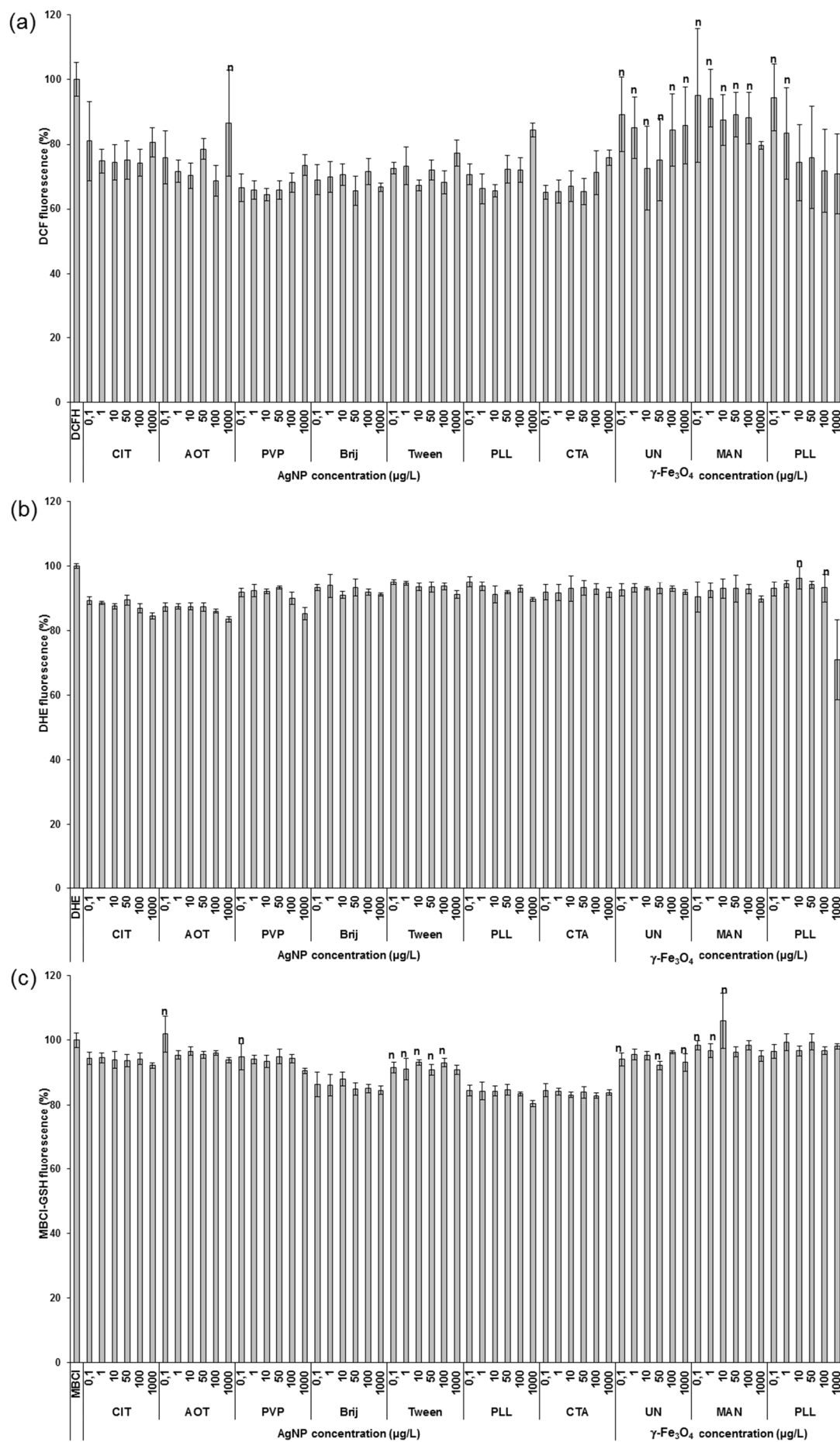


Figure 6. The effect of different concentrations of AgNPs and γ -Fe₂O₃NPs with different surface coating on DCFH-DA (a), DHE (a) and MBCl (c) assays after 45 min of incubation at 37 °C. ⁿ indicates values that were not significantly different from the control (fluorescent probes alone), while all other values were significantly different from the control at $P < 0.05$.

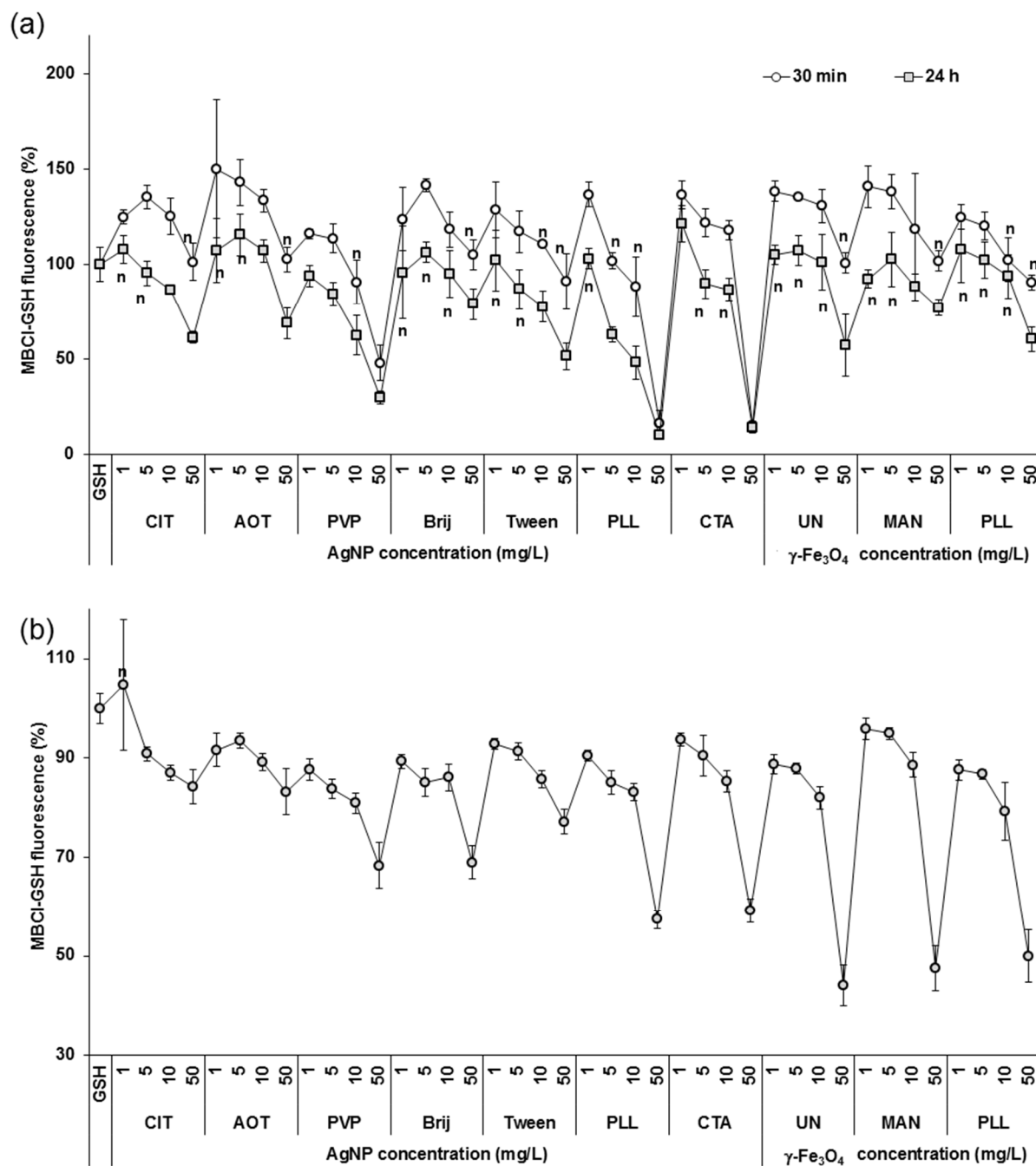


Figure 7. The effect of different concentrations of AgNPs and $\gamma\text{-Fe}_2\text{O}_3$ NPs with different surface coating on MBCl-GSH adduct formation. (a) The MBCl, GSH and NPs were mixed and fluorescence was measured after 30 min (white circle) and 24 h (grey cubes) after incubation at 37 °C. (b) The GSH was incubated with NPs for 2 h and fluorescence was measured 30 min after addition of MBCl. ⁿ indicates values that were not significantly

different from the control (MBCl + GSH), while all other values were significantly different from the control at $P < 0.05$.

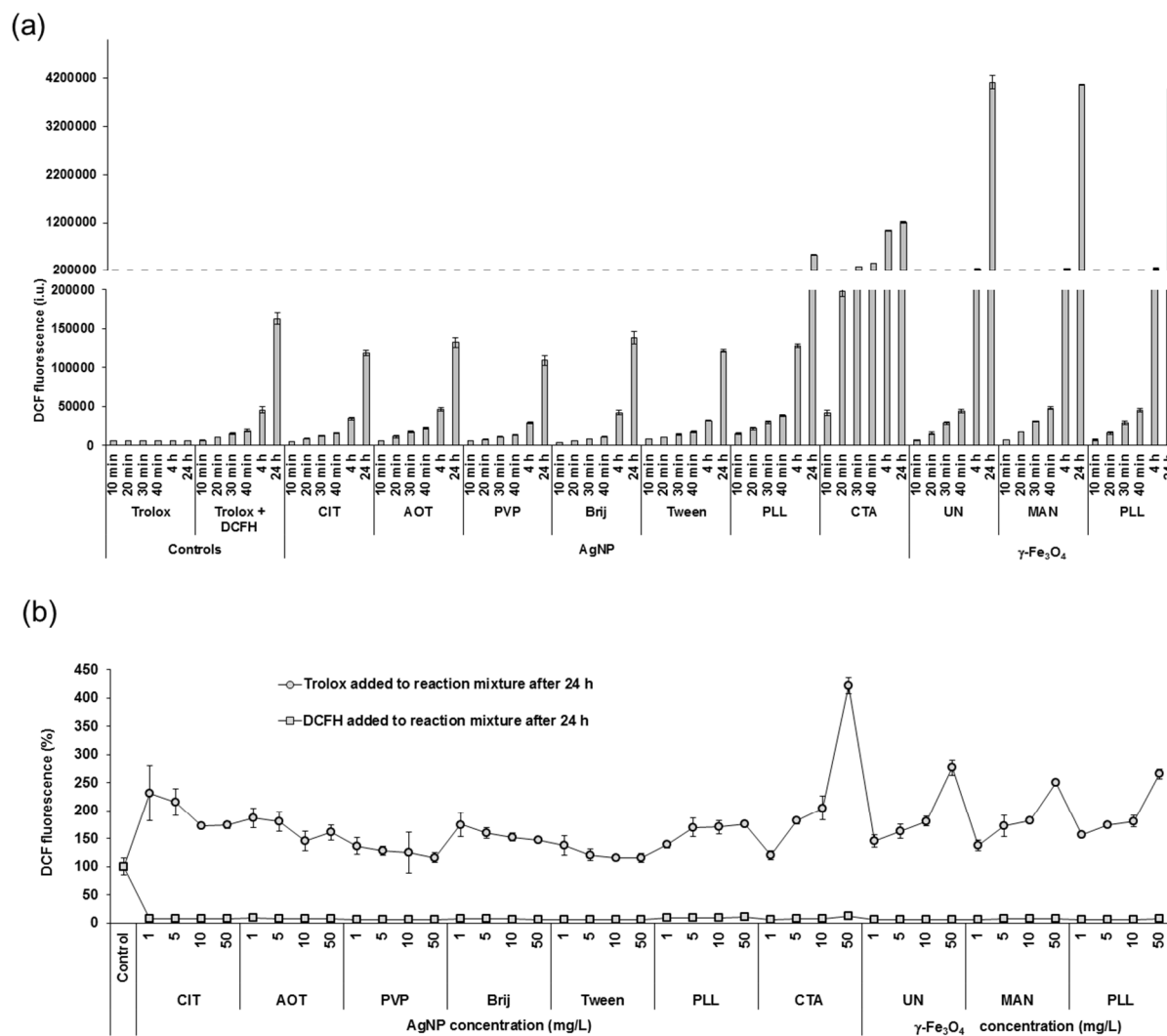


Figure 8. The effect of different concentrations of AgNPs and $\gamma\text{-Fe}_2\text{O}_3$ NPs with different surface coating on oxidation of DCFH with Trolox. (a) The NPs were incubated with Trolox and DCFH, and fluorescence was measured after 10, 20, 30, 40 min, 4 and 24 h. (b) The NPs were incubated with Trolox (grey circle) or DCFH-DA (grey cubes) for 24 h at 37 °C, and fluorescence was measured after the addition of DCFH or Trolox, respectively. All values were significantly different from the control (Trolox + DCFH-DA) at $P < 0.05$.

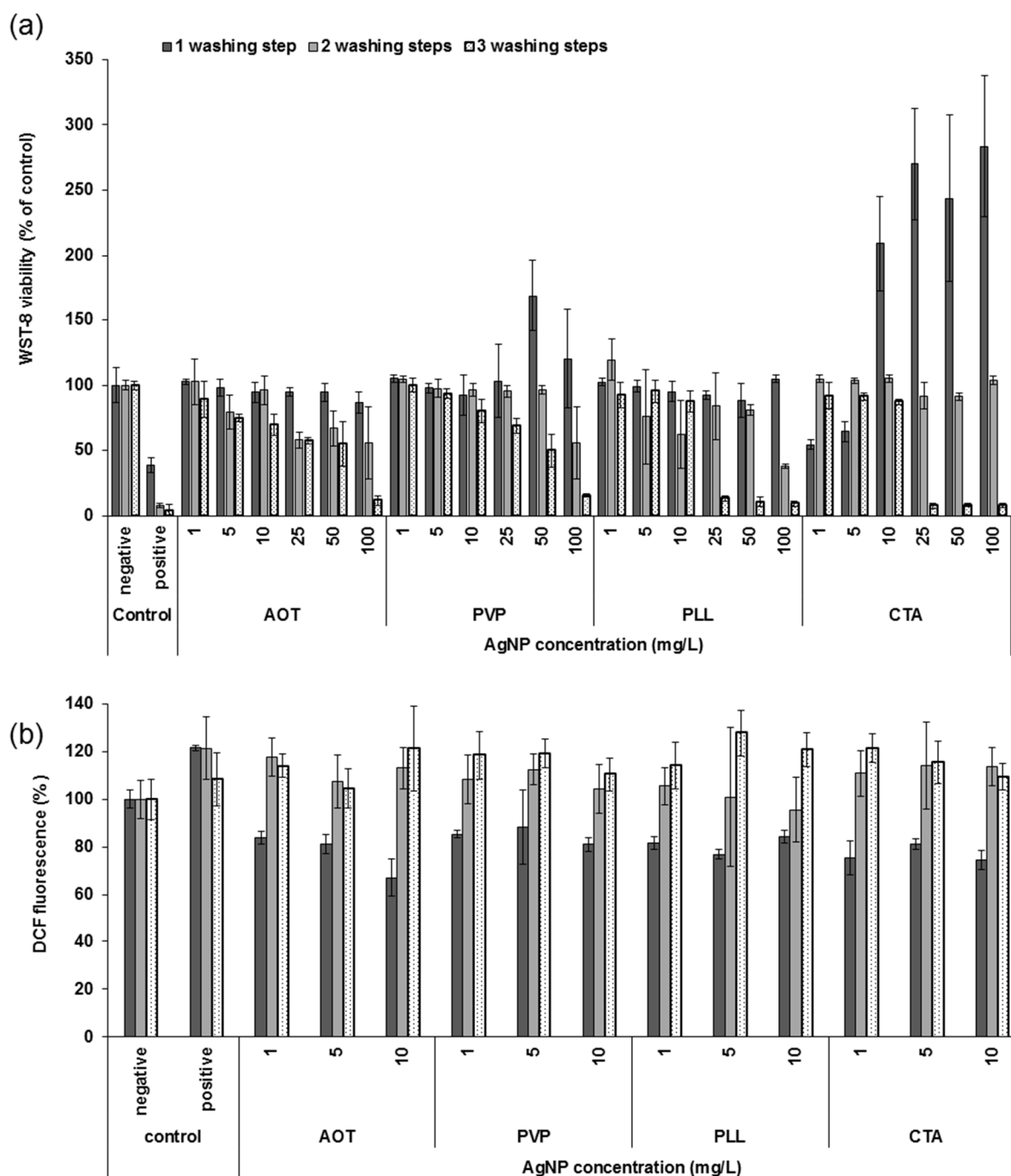


Figure 9. The effect of 1-3 washing steps on cell viability and ROS level in HepG2 cell treated with different concentrations of differently coated AgNPs. (a) The cell viability was employed using WST-8 assay. Negative control was cells in DMEM, while positive control was cells treated with DMSO. (b) ROS level measured by DCFH-DA assay. Negative control was cells in DMEM, while positive control was cells treated with 100 μ M hydrogen peroxide.